Components Irradiation Test 7

prepared for

George C. Marshall Space Flight Center / NASA

Georgia Nuclear Laboratories

LOCKHEED-GEORGIA COMPANY -- A Division of Lockheed Aircraft Corporation

LOCKHEED

ER 7620

COMPONENTS IRRADIATION TEST NO. 7
2N834 TRANSISTORS
1N540 AND 1N649 DIODES
S1N752A ZENER DIODES

28 SEPTEMBER 1964

Prepared For:

GEORGE C. MARSHALL SPACE FLIGHT CENTER

Prepared By:

GEORGIA NUCLEAR LABORATORIES

GEORGIA NUCLEAR LABORATORIES
Lockheed-Georgia Company – A Division of Lockheed Aircraft Corporation

Contract NAS 8-5332
Code U

FOREWORD

This report is submitted to the Astrionics Laboratory of the George C. Marshall Space Flight Center, National Aeronautics and Space Administration, Huntsville, Alabama, in accordance with the requirements of Task Order No. ASTR-LGC-16 of Contract No. NAS 8-5332. The report is one of a series describing radiation effects on various electronic components. This particular report concerns transistors, diodes and Zener diodes. The tests were performed by the Georgia Nuclear Laboratories, Lockheed-Georgia Company.

TABLE OF CONTENTS

LIST OF TABLES AND FIGURES

LIST OF TABLES AND FIGURES

(Continued)

LIST OF TABLES AND FIGURES

(Continued)

1.0 SUMMARY

One type of transistor with specimens from each of three manufacturers, two types of diodes, and one type of Zener diode were subjected to a radiation environment in a controlled temperature chamber to determine the effect of radiation on selected component parameters.

Failure criteria for the test were: (1) A 50% reduction in h_{FE} of the transistor specimens, (2) a 100% increase in V_F, or an increase in I_R beyond specified maximum values, for the diodes.

Results of the test were:

1. All transistor specimens failed. Median radiation exposure levels were as follows:

		50% Failed At		
Type	Manufacturer	n/cm^2	plus	r
2N834	Motorola	2.8×10^{13}		8.1×10^5
2N834	General Electric	3.4×10^{13}		8.6×10^5
2N834	Fairchild	5.0×10^{13}		9.3×10^5

2. The h_{ie} parameter of the transistors decreased in the same manner as the h_{FE}.
3. Except for a few specimens, the I_{CBO} of the transistors did not change.
4. The majority of the 1N540 diodes failed because of increased I_R while the remainder failed because of increased V_F.
5. All of the 1N649 diodes failed because of increased V_F.
6. A very slight increase in the V_Z of the S1N752A Zener diodes was noted.

2.0 INTRODUCTION

The experiment described in this report is the seventh irradiation of electronic components and is the eleventh in a series of radiation effects tests on electronic equipment, circuits, and components contemplated for use on a nuclear space vehicle. Since the use of equipment on this vehicle is contingent upon its ability to withstand the nuclear environment, the Astrionics Laboratory of the Marshall Space Flight Center has undertaken to assure that Government furnished or specified equipment will survive this environment. The equipment is to be subjected to the expected nuclear environment as simulated at the Georgia Nuclear Laboratories. Measurements made on the equipment during the irradiation will describe its radiation tolerance.

The subjects of this test are the type 2N834 transistor, the types 1N540 and 1N649 diodes, and the type S1N752A Zener diode.

3.0 TEST PROCEDURE

The test specimens were supplied by the Astrionics Laboratory of the George C. Marshall Space Flight Center. They were exposed to a nominal gamma dose of 6.1×10^5 r behind a neutron attenuator shield. The shield was removed and the test continued to a nominal integrated neutron flux of 1.1×10^{15} n/cm^2. During the test, the semiconductor specimens were mounted in a controlled temperature chamber at $45 \pm 2^\circ$ C. Before, during and after the irradiation, measurements were made to determine the parameters listed in Table 1. Measurements were also made during the test to define the nuclear and temperature environments.

3.1 TEST SPECIMENS

The specimens tested are listed in Table 1. These specimens were mounted by the Astrionics Laboratory. All specimens were new units and had only been subjected to MSFC receiving inspection. Manufacturer's specifications for these specimens are tabulated in Table 2. The specimens were soldered on printed circuit boards which were mounted vertically on the test panel to equalize the radiation flux distribution. Figures 1 and 2 show the relative positions of the specimen mounting boards. The test fixture as shown in Figure 1 was placed directly adjacent to the reactor for the irradiation with the environment chamber cover in place.

3.2 TEST SPECIMEN MEASUREMENTS

A complete set of data was taken prior to reactor startup to establish baseline data for the test. During the irradiation, measurements were made at all reactor power settings. Measurements were also made: (a) during reactor shutdown for removal of the shield; (b) immediately after reactor shutdown upon completion of irradiation; and (c) approximately ten hours after completion of irradiation (on non-failed specimens). All measurements were performed with the test fixture in place at the reactor facility.

3.3 INSTRUMENTATION

3.3.1 Transistor Measurement Circuits

The transistor measurement circuits are shown in Figures 3 and 4. The emitters of each transistor test specimen were commoned and the base and collector were commutated into the test circuits. In the h_{FE} and the h_{ie} measurement circuit, Figure 3, the feed-back loop including amplifier "A" establishes the base current necessary to provide a collector current of 10 ma. 910 pF capacitors were connected from collector to emitter of each specimen at the mounting board to prohibit an oscillation caused by the inductance and capacitance of the long lines. These are mica capacitors and have previously been shown to be tolerant of the radiation levels experienced in this test. The base current is measured by the digital voltmeter and h_{FE} is calculated from these measurements. With a signal current of 10 μa at 1 kc applied to the base, the base to emitter voltage (V_{be}) is measured by an ac voltmeter. The dc output of this meter is monitored by the digital voltmeter and these values are used in determination of the input impedance (h_{ie}). The system sensitivity of the I_{CBO} measurement circuit, Figure 4, was in the order of 10^{-9} amps. System accuracy was $\pm$ 1% $\pm$ 10 nA.

3.3.2 Diode Measurement Circuits

The circuits, Figures 5, 6, and 7, were used to perform the diode measurements with the GNL ACMS. The cathodes of all diodes were commoned and the anodes were commutated into the test circuits. Potential leads for the diode specimens were used to eliminate the voltage drop in the 300-foot instrumentation cables to the test specimens. The parameters measured for the different types are shown in Table 1.

3.4 TEST ENVIRONMENT

3.4.1 Pressure

The test was conducted at atmospheric pressure.

3.4.2 Temperature

The transistor and diode specimens were located in the environmental chamber at a temperature of 45 $\pm 2^{o}$ C throughout most of the test. See Figure 8 for temperature environment during the test. A combination of gamma heating and high ambient temperature caused a rise in environmental chamber temperature near the end of the irradiation.

3.4.3 Nuclear

The irradiation was performed in two radiation phases with a lapse of about 1 hour between phases. The first phase was conducted with a lithium hydride shield interposed between test specimens and the reactor. The second phase was conducted without shielding. The neutron to gamma ratio behind the shield was about 2×10^{5} nvt/r, as compared to about 10^{8} nvt/r without the shield. During the irradiation both neutron and gamma radiation were monitored and recorded.* Isoline radiation flux plots were made for the test panels and used in the data reduction.

*A more detailed description of the GNL Nuclear Measurement System is contained in a previous report; viz Components Irradiation Test No. 1, ER 6785, Georgia Nuclear Laboratories, Dawsonville, Georgia.

4.0 METHOD OF DATA ANALYSIS

The GNL Data Logging System recorded the parameter measurements in typewritten digital form and simultaneously punched the data in 5-channel perforated tape. A tape-to-card converter was used to transfer the h_{FE} and h_{ie} data to IBM cards which were then programmed into an IBM 7094 computer to yield h_{FE}, h_{FE_n} (normalized h_{FE}), h_{ie}, and h_{ie_n} (normalized h_{ie}). Normalization was accomplished by dividing each parameter value by its corresponding pre-irradiation value.

The mean parameter value for a data group, where shown, was computed by adding the individual specimen parameter values and dividing the sum by the number of specimens.

The median parameter value for a data group (that value which divides a distribution so that an equal number of items is on either side of it) was determined from a plot of the individual specimen parameter values on an arithmetic probability chart. The limits of the 68% envelopes were determined by picking off those values within which were contained 34% of the specimens next above the group median value and 34% of the specimens next below the group median value. The limits of the 95% envelope were found in a similar fashion. The 7094 computer performed these functions for the h_{FE} and h_{ie} parameters. The median and envelope limits for other parameters were determined graphically in the same manner.

In those cases where the parameter of an individual specimen behaved significantly differently from the group median, these "unusual" specimens have been portrayed in separate figures.

Radiation environmental data shown on the figures' abscissae were obtained by integrating, with respect to time, the gamma dose rates and neutron flux rates.

Those figures which show "Percent Failed Versus Integrated Neutron Flux" were prepared after the procedure described by Mr. Frank W. Poblenz in an article entitled "Analysis of Transistor Failure in a Nuclear Environment," which appeared in Volume NS-10, Number 1, January 1963, of the IEEE Transactions on Nuclear Science. This type of presentation enables the circuit designer to predict the radiation level at which any given percentage of the particular component will equal or exceed the failure criteria.

Copies of the reduced data from which the graphs were prepared are on file in the Astrionics Laboratory of the George C. Marshall Space Flight Center, NASA, Huntsville, Alabama, and in the Georgia Nuclear Laboratories, Lockheed-Georgia Company, Dawsonville, Georgia.

5.0 TEST DATA AND DISCUSSION OF RESULTS

The test data have been presented herein in graphical form. The radiation exposure is, in all cases, a combination of neutrons and gammas. The abscissa scale on each of the graphs is accumulated neutrons/cm^2 greater than 0.5 MeV. However, the coincident accumulated gamma dose (r) is also indicated at those points where changes in the reactor power rate occurred. It is important to remember that the total radiation exposure consists of both neutrons and gammas, and that each may contribute, in varying degrees, to the degradation of a component's parameter.

5.1 TYPE 2N834 TRANSISTOR

5.1.1 The h_{FE} Parameter

The h_{FE} of all specimens tested was decreased by the irradiation. The patterns of degradation for each of the three manufacturers are shown in Figures 9, 10, and 11. The patterns are similar in that each shows a discontinuity at the point of shield removal. This appears to indicate that gamma radiation is a significant factor in the loss of h_{FE}. The dispersion of the normalized h_{FE} values about the median value was essentially the same for the General Electric and Motorola specimens, but was noticeably less for the Fairchild specimens.

Figures 12, 13, and 14 show the failure patterns for the three groups. The criterion for failure was a 50% reduction in h_{FE}. Figure 15 is a composite of the three preceding figures to facilitate comparison. From this figure it can be seen that the Motorola specimens exhibited the least tolerance to radiation while the Fairchild specimens showed the greatest.

Initial values of h_{FE} and order of failure are shown for each specimen as follows:

GENERAL ELECTRIC

h_{FE_o}	Order of Failure
50.66	9
52.35	32
52.36	22
54.20	13
54.92	25
56.80	18
57.57	23
58.37	4
58.48	27
58.72	11
58.82	28
59.73	2
59.95	29
60.20	21
60.53	3
60.83	24
61.58	20
61.71	16
61.88	1
62.07	17
62.39	10
64.09	19
66.27	5
70.30	31
73.50	26
74.22	12

GENERAL ELECTRIC (Continued)

h_{FE_o}	Order of Failure
75.15	6
76.10	14
76.80	30
78.10	15
82.93	8
87.71	7

There is a very slight correlation between high h_{FE_o} and early failure in these data.

MOTOROLA

h_{FE_o}	Order of Failure
62.86	28
66.19	31
66.64	33
70.25	32
72.01	29
73.72	39
75.69	26
77.51	30
79.59	38
79.78	23
81.27	37
82.24	40
82.81	20
83.13	18

MOTOROLA (Continued)

h_{FE_o}	Order of Failure
83.27	22
83.33	21
83.48	34
85.61	19
86.65	24
89.49	27
99.57	35
102.40	9
108.40	36
117.60	10
140.00	12
140.80	7
158.70	4
161.00	14
162.60	6
177.10	3
178.50	8
185.00	25
187.90	5
188.30	15
197.20	1
204.00	13
207.90	17
209.20	11
210.00	16
275.40	2

In these data there is excellent correlation between high h_{FE_o} and early failure.

FAIRCHILD

h_{FE_o}	Order of Failure
34.66	34
42.00	36
42.53	27
43.33	25
44.63	11
46.42	32
48.95	35
58.31	23
58.81	21
59.13	24
59.69	3
59.88	26
60.12	16
60.61	15
61.53	13
62.11	9
63.89	30
64.38	4
64.79	33
65.33	14
65.58	20
66.65	2
66.78	19
67.23	6
67.57	12
69.79	28
70.57	37

FAIRCHILD (Continued)

h_{FE_o}	Order of Failure
70.62	7
70.71	8
71.51	18
71.91	31
72.31	5
72.54	1
73.40	17
73.42	22
75.75	29
77.50	10

These data indicate a slight correlation between high h_{FE_o} and early failure.

5.1.2 The h_{ie} Parameter

Figures 16, 17, and 18 show the normalized h_{ie} data for each of the three groups of specimens. The similarity of these figures to the corresponding figures showing the normalized h_{FE} data (Figures 9, 10, and 11) may be explained by the relationship:

$$h_{ie} = r_{bb} + h_{fe}\, r_e$$

where r_{bb} = base spreading resistance

and r_e = emitter junction resistance

Since $h_{fe} \approx h_{FE}$ the expression may be written $h_{ie} \approx r_{bb} + h_{FE}\, r_e$. Normally $h_{FE}\, r_e$ (or $h_{fe}\, r_e$) is the predominant factor and thus controls h_{ie}.

5.1.3 The I_{CBO} Parameter

Except for the "unusual" specimens shown in Figures 19, 20, and 21 no increase in I_{CBO} was detected for any of the specimens. Small increases did occur in the data obtained but these were attributed to radiation rate effects in the instrumentation cables. The data shown in Figures 19, 20, and 21 have been corrected for cable effects. The mean I_{CBO} values and the range of values obtained in pre-test measurements are shown below for each group:

	Pre-Test I_{CBO} Values (μa)	
Group	Mean*	Range*
General Electric	.028	.01 - .07
Motorola	.035	.02 - .05
Fairchild	.014	.01 - .04

*Less "unusual" specimens

5.2 TYPE 1N540 DIODE

5.2.1 The V_F Parameter

Figure 22 shows the behavior of V_F at I_F = 250 ma while Figure 23 shows V_F at I_F = 500 ma. The patterns in the two figures are practically identical. In both cases V_F began increasing at about 2×10^{11} n/cm^2 and continued to rise at an increasing rate as the irradiation continued. Figures 24 and 25 show the failure patterns for one of the failure criteria selected, i.e., $V_F/V_{F_o} \geq 2$. There appears to be no significant difference between the two patterns. As will be shown in the following paragraph, all but seven of the specimens failed due to increase in I_R before failure due to increase in V_F.

5.2.2 The I_R Parameter

Under the failure criteria selected for these diodes ($V_F/V_F \geq 2$ or $I_R > 200\ \mu a$) thirteen of the specimens failed due to increase in I_R. The I_R data for the group are shown in Figure 26. I_R of some of the specimens began to increase at about 10^{10} n/cm^2 and showed a rapid rise thereafter. For other specimens there was comparatively little change in I_R prior to failure because of increased V_F. Figure 27 shows the I_R data for the eight specimens with the smaller changes in I_R. Figure 28 shows the failure pattern for the 13 specimens which failed because of increased I_R. The spread of data would indicate that few, if any, conclusions could be drawn. The last two failures did not fit the pattern of the first eleven. This may indicate that at least two modes of failure are involved. One of these may be surface effects.

5.3 TYPE 1N649 DIODE

5.3.1 The V_F Paramater

The V_F data for I_F values of 200 ma and 400 ma are shown in Figures 29 and 30 respectively. V_F at I_F=400 ma began a noticeable increase slightly before V_F at I_F = 200 ma. However, Figures 31 and 32 show no significant difference in the failure patterns of the two test conditions.

5.3.2 The I_R Parameter

Figure 32 shows the I_R data for this type diode. There was an increase in I_R which appeared to be a function of both radiation rate and radiation exposure. The rate effect was most noticeable at the higher neutron rates. There was considerable annealing during the period of reactor shutdown for shield removal with the median I_R value dropping below the pre-test median value.

5.4 TYPE S1N752A ZENER DIODE

5.4.1 The V_Z Parameter

Figure 33 shows a slow but steady increase in V_Z during the irradiation. The total increase in the median value amounted to about 0.35%. The post test measurements taken approximately 10 hours after reactor shutdown showed some annealing of this parameter. Pre-test V_Z values ranged from 5.5658V to 5.8065V. Post-test V_Z values ranged from 5.5903V to 5.8221V.

TABLE 1 TEST SPECIMENS AND TEST CONDITIONS

Board No.	Description	No. Tested	Test Conditions	Parameter
1 & 2	Transistor, 2N834 NPN, Si, General Electric	40	$V_{CB} = 10V, I_E = 0$ $V_{CE} = 1.0V, I_C = 10$ ma $V_{CE} = 1.0V, I_C = 10$ ma $I_{Sig} = 10\ \mu a$ at 1 kc	I_{CBO} h_{FE} h_{ie}
3 & 4	Transistor, 2N834 NPN, Si, Motorola	40	$V_{CB} = 10V, I_E = 0$ $V_{CE} = 1.0V, I_C = 10$ ma $V_{CE} = 1.0V, I_C = 10$ ma $I_{Sig} = 10\ \mu a$ at 1 kc	I_{CBO} h_{FE} h_{ie}
5 & 6	Transistor, 2N834 NPN, Si, Fairchild	40	$V_{CB} = 10V, I_E = 0$ $V_{CE} = 1.0V, I_C = 10$ ma $V_{CE} = 1.0V, I_C = 10$ ma $I_{Sig} = 10\ \mu a$ at 1 kc	I_{CBO} h_{FE} h_{ie}
7	Diode, 1N540 General Electric	20	$I_F = 250$ ma $I_F = 500$ ma $V_R = 400$ VDC	V_F V_F I_R
9	Diode, 1N649 General Electric	20	$I_F = 200$ ma $I_F = 400$ ma $V_R = 400$ VDC	V_F V_F I_R
8	Diode, Zener S1N752A Motorola	20	$I_{ZT} = 20$ ma	V_Z

TABLE 2 MANUFACTURERS' SPECIFICATIONS FOR TEST SPECIMENS

Test Specimens	Conditions	Specifications
Transistor 2N834	$V_{CE} = 1.0V$, $I_C = 10$ ma $V_{CB} = 20V$, $T = 25^\circ$ C $V_{CB} = 20V$, $T = 150^\circ$ C	$h_{FE} = 25$ min, 40 typical $I_{CBO} = 0.5$ μa max. $I_{CBO} = 30$ μa max.
Diode 1N540	$I_F = 500$ ma, $T = 25^\circ$ C $V_R = 400V$, $T = 25^\circ$ C $V_R = 400V$, $T = 150^\circ$ C	$V_F = 1.0$ VDC $I_R = 10$ μa max. $I_R = 200$ μa max.
Diode 1N649	$I_F = 400$ ma, $T = 25^\circ$ C $V_R = 600$ VDC, $T = 25^\circ$ C $V_R = 600$ VDC, $T = 100^\circ$ C	$V_F = 1.0$ VDC $I_R = 0.2$ μa max. $I_R = 25$ μa max.
Zener Diode S1N752A	$I_{ZT} = 20$ ma	$V_Z = 5.6V$

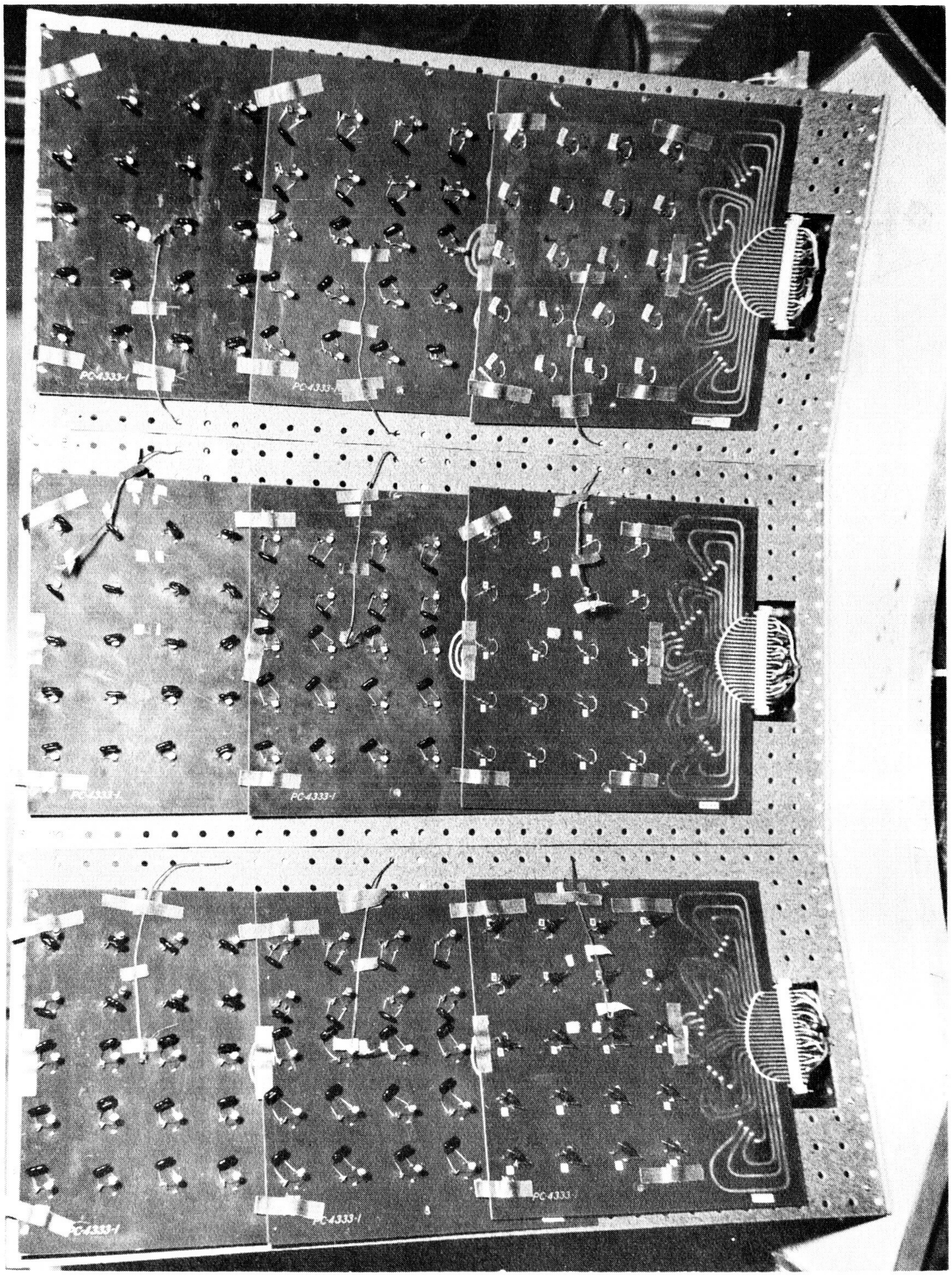

FIGURE 1 TEST PANEL AS SEEN FROM REACTOR

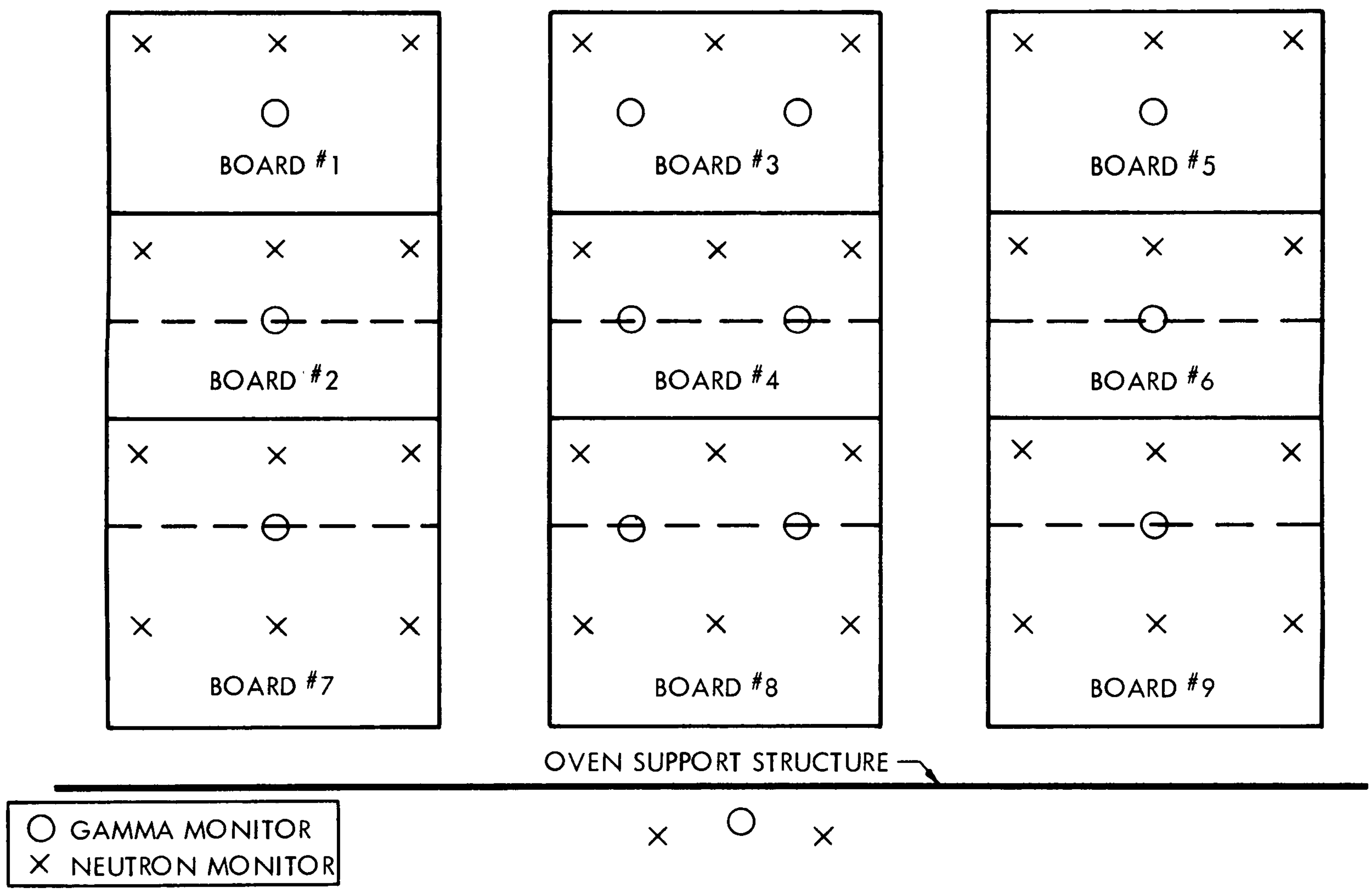

FIGURE 2 DIAGRAM OF TEST PANEL AS SEEN FROM REACTOR

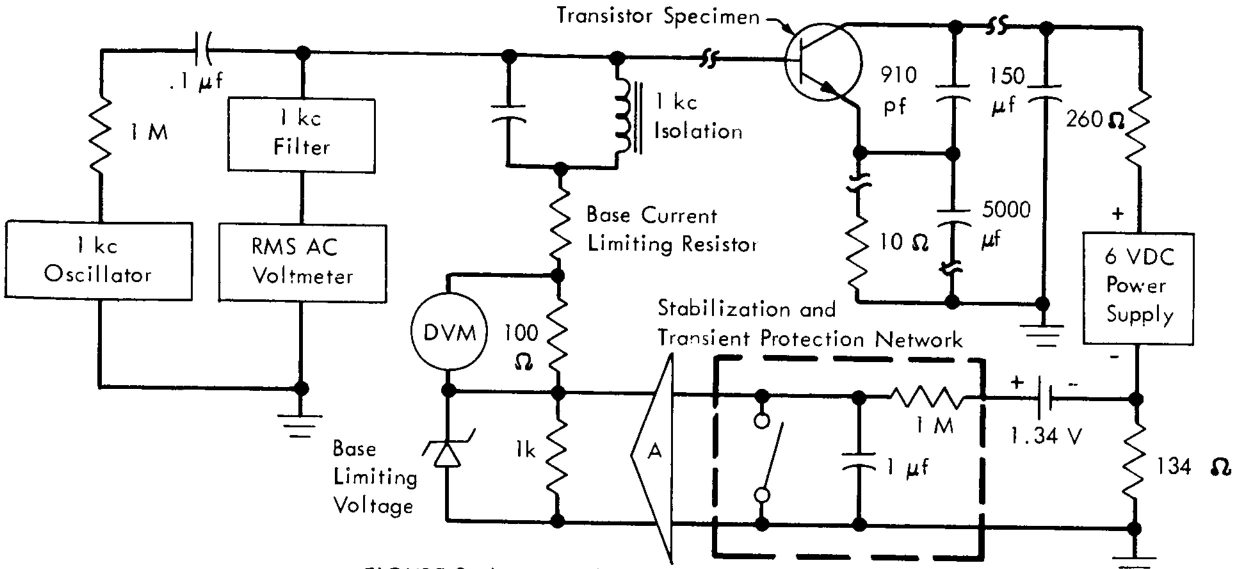

FIGURE 3 h_{FE} AND h_{ie} MEASURING CIRCUIT

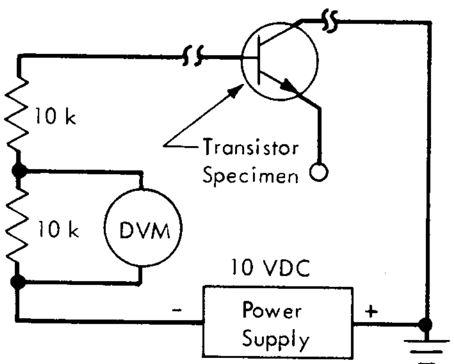

FIGURE 4 I_{CBO} MEASURING CIRCUIT

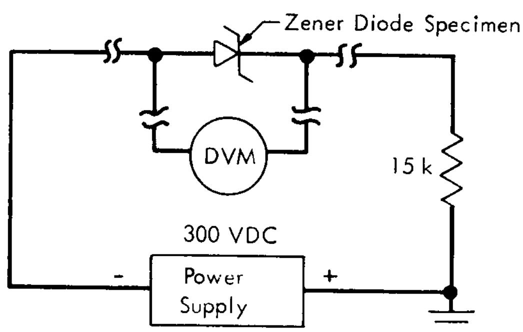

FIGURE 5 V_Z MEASURING CIRCUIT

Diode	E	R	I_F
IN250	60 VDC	210 Ω	250 ma
	60 VDC	100 Ω	500 ma
IN649	60 VDC	265 Ω	200 ma
	60 VDC	128 Ω	400 ma

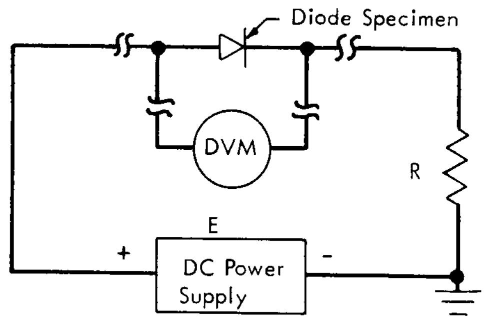

FIGURE 6 V_F MEASURING CIRCUIT

Diode	V_R
IN250	400 VDC
IN649	400 VDC

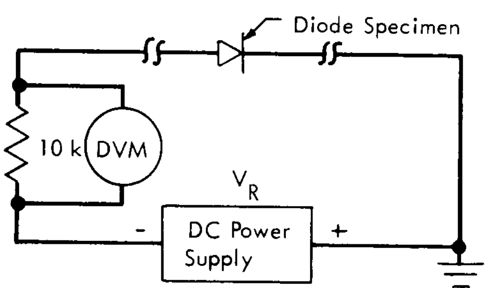

FIGURE 7 I_R MEASURING CIRCUIT

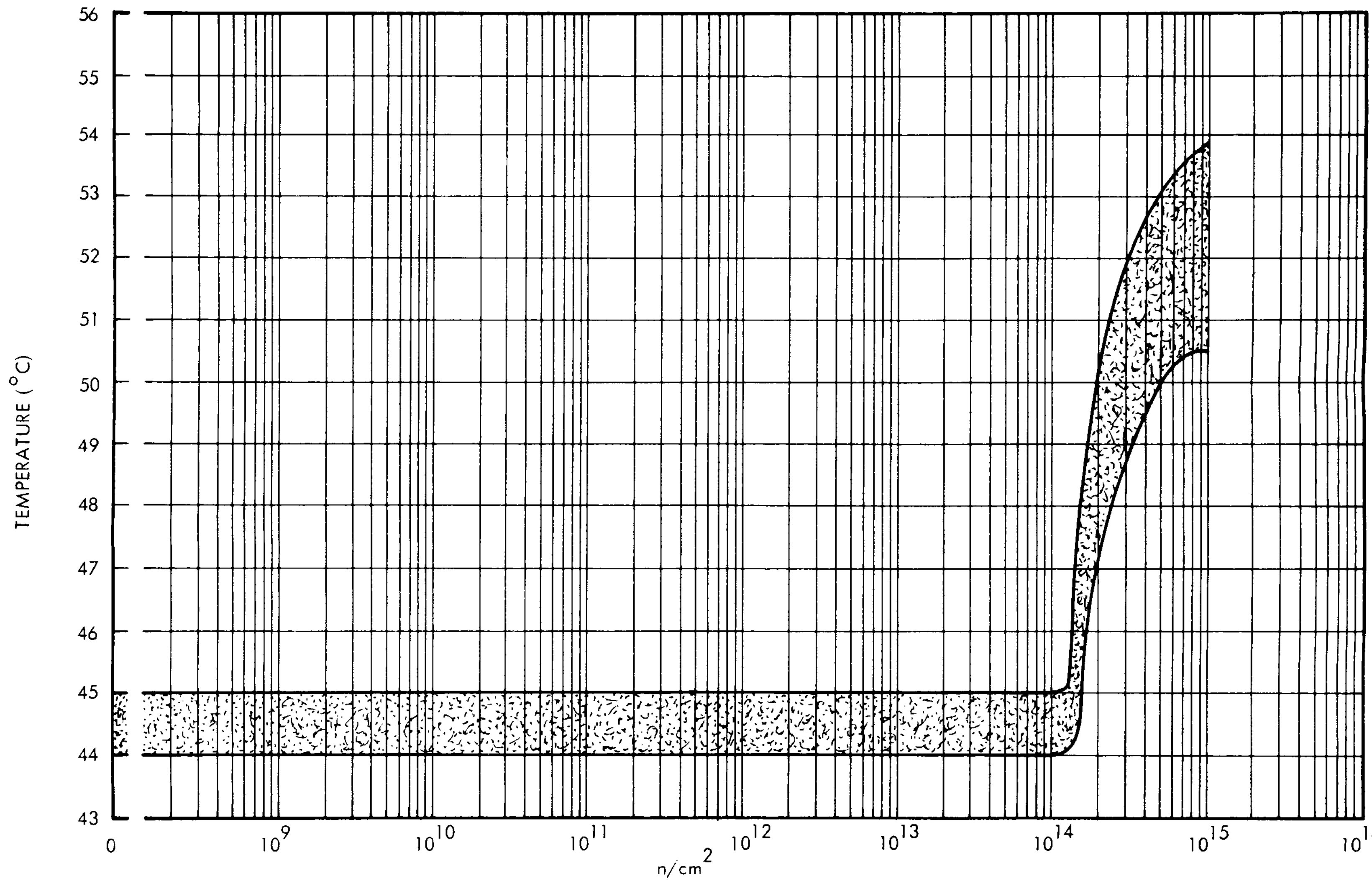

FIGURE 8 RANGE OF SPECIMENS' TEMPERATURES VERSUS INTEGRATED NEUTRON FLUX

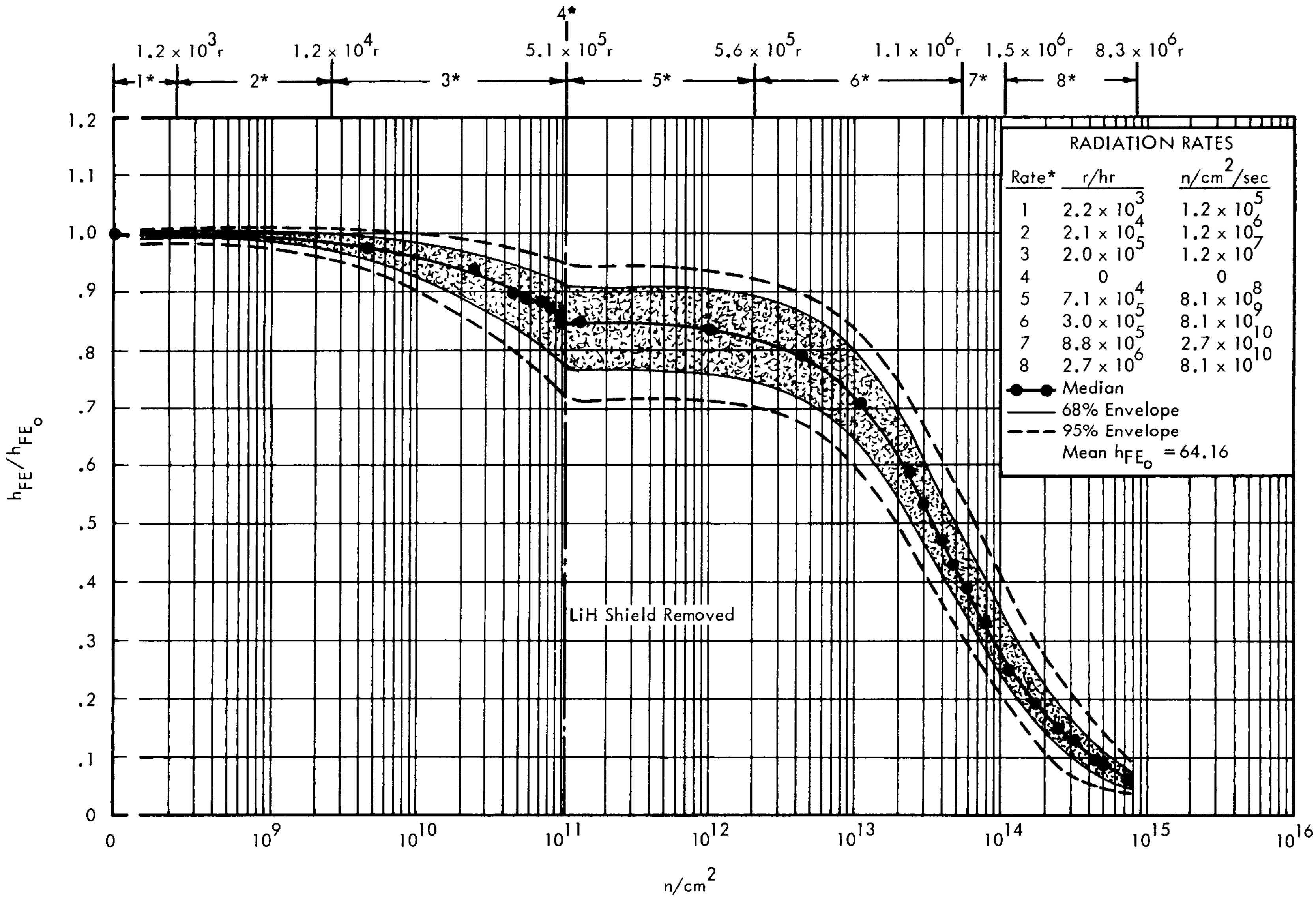

FIGURE 9 2N834, GENERAL ELECTRIC, 45° C, NORMALIZED h_{FE} VERSUS INTEGRATED NEUTRON FLUX

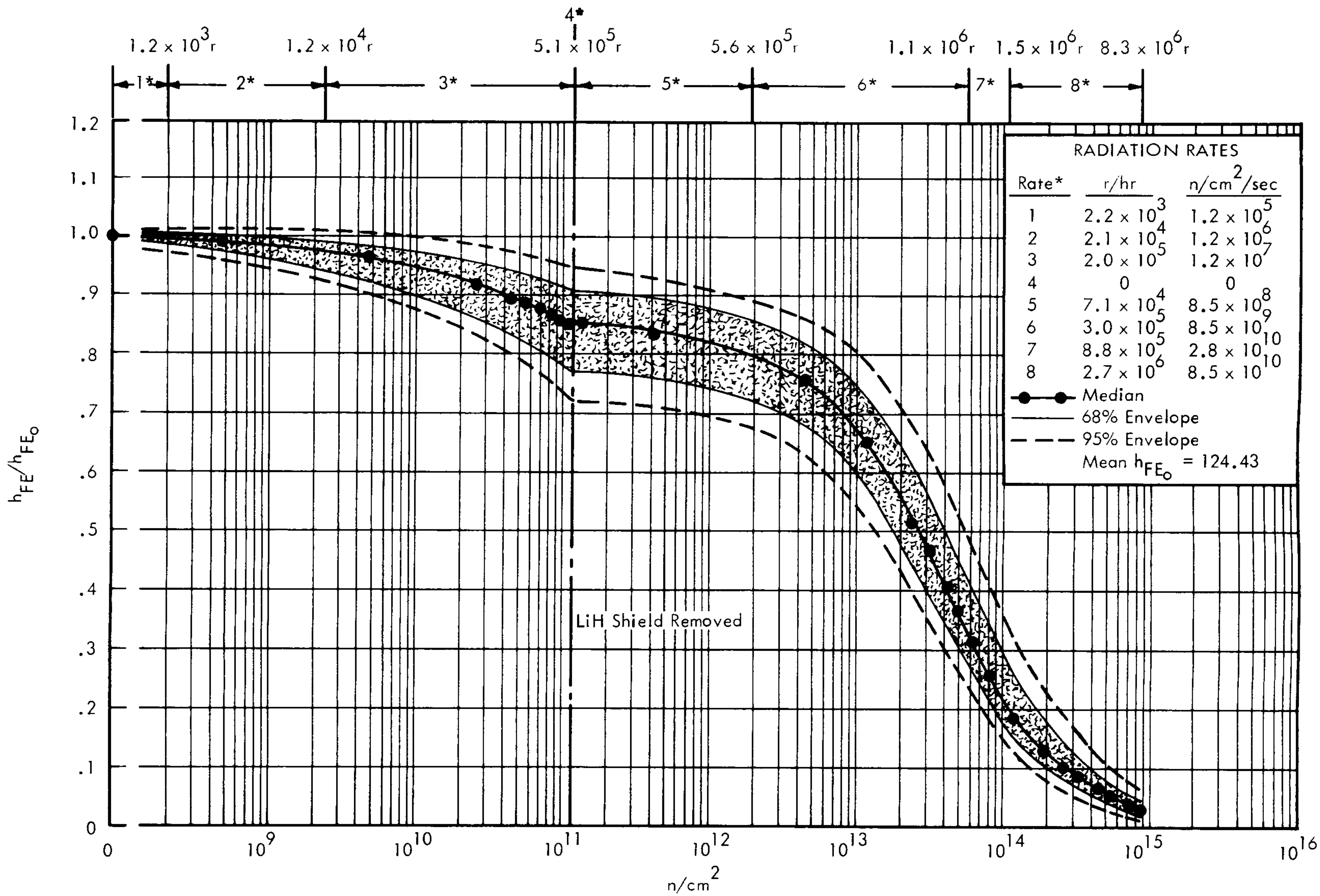

FIGURE 10 2N834, MOTOROLA, 45° C, NORMALIZED h_{FE} VERSUS INTEGRATED NEUTRON FLUX

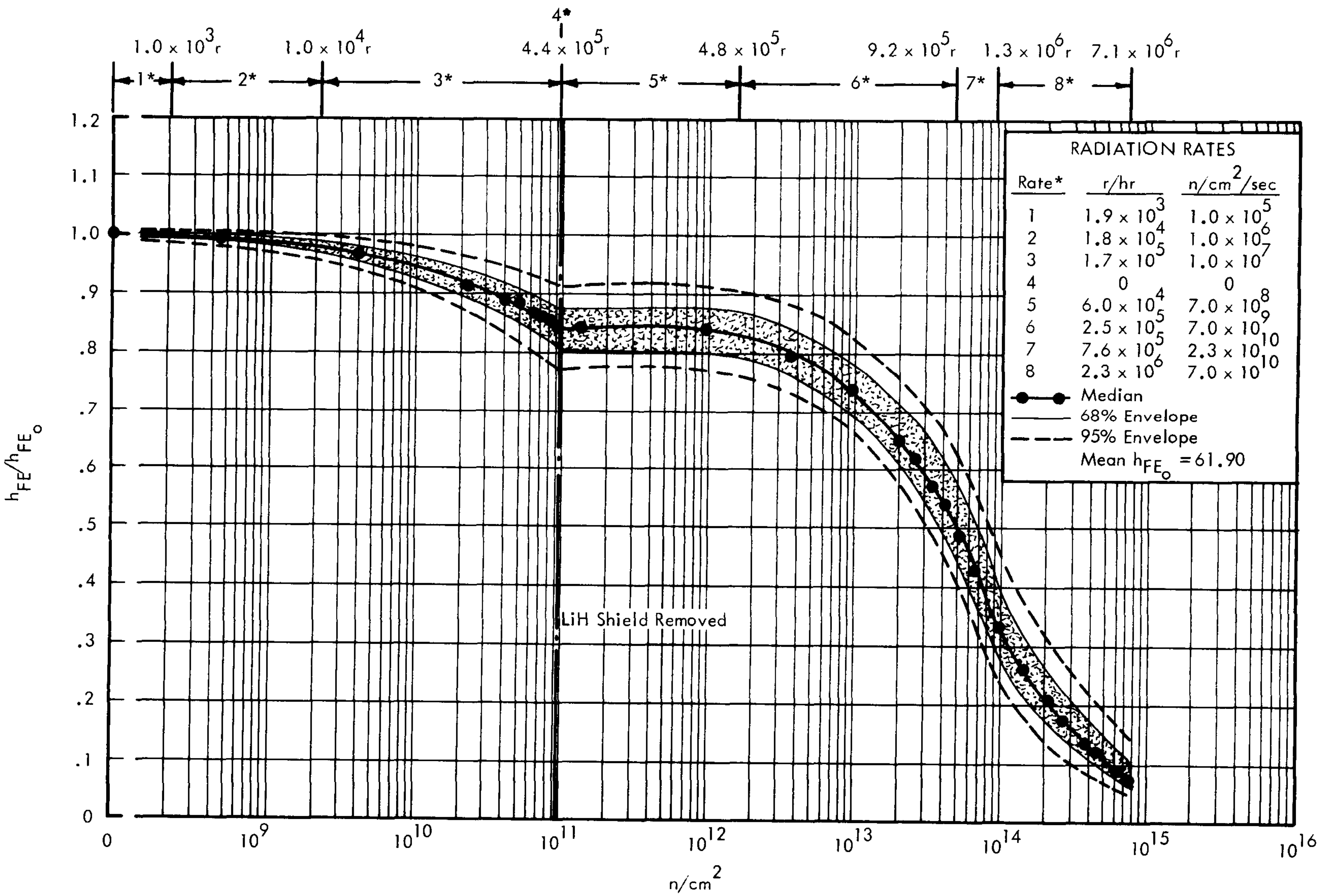

FIGURE 11 2N834, FAIRCHILD, 45° C, NORMALIZED h_{FE} VERSUS INTEGRATED NEUTRON FLUX

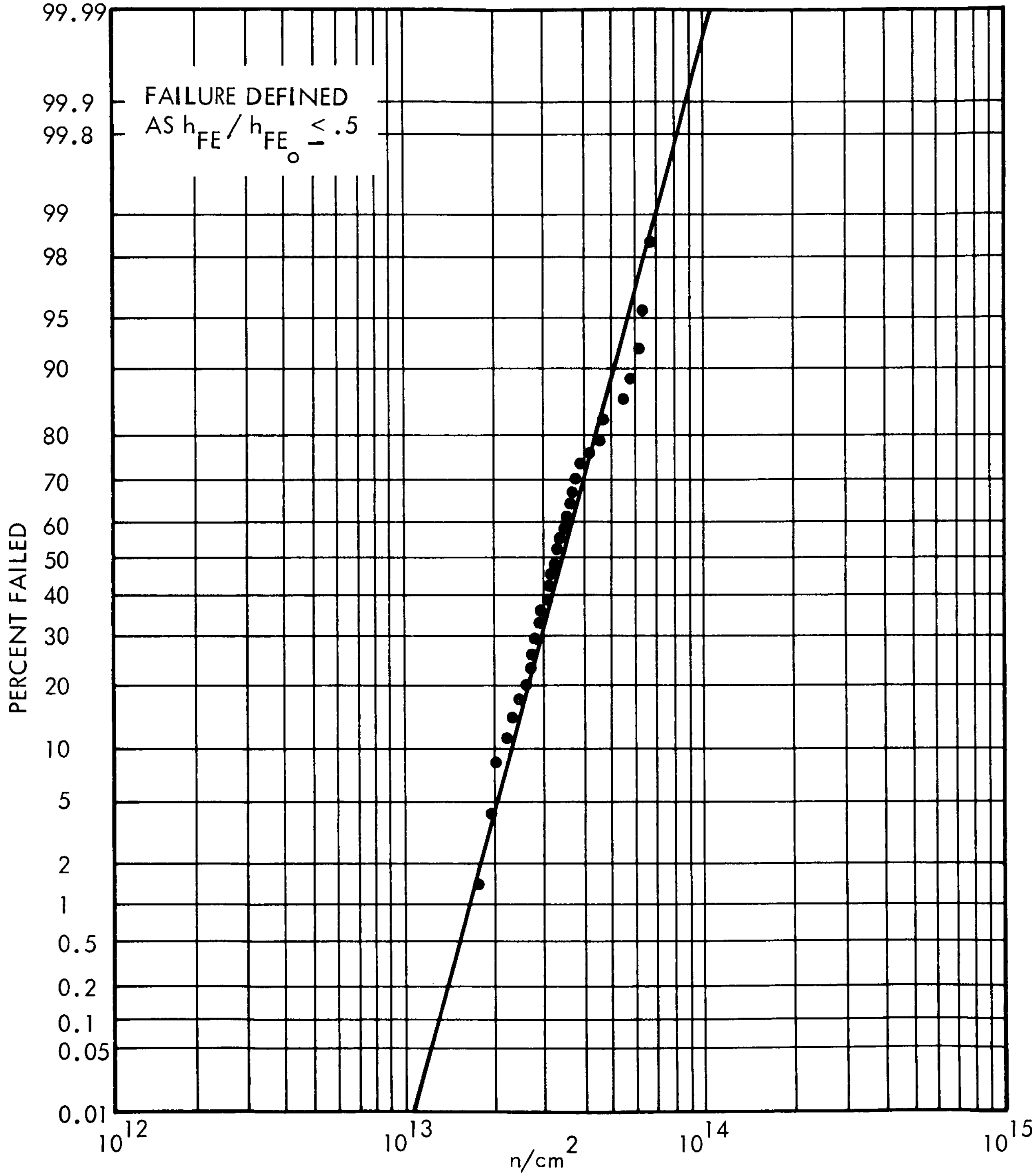

FIGURE 12 2N834, GENERAL ELECTRIC, 45° C, PERCENT FAILED VERSUS INTEGRATED NEUTRON FLUX

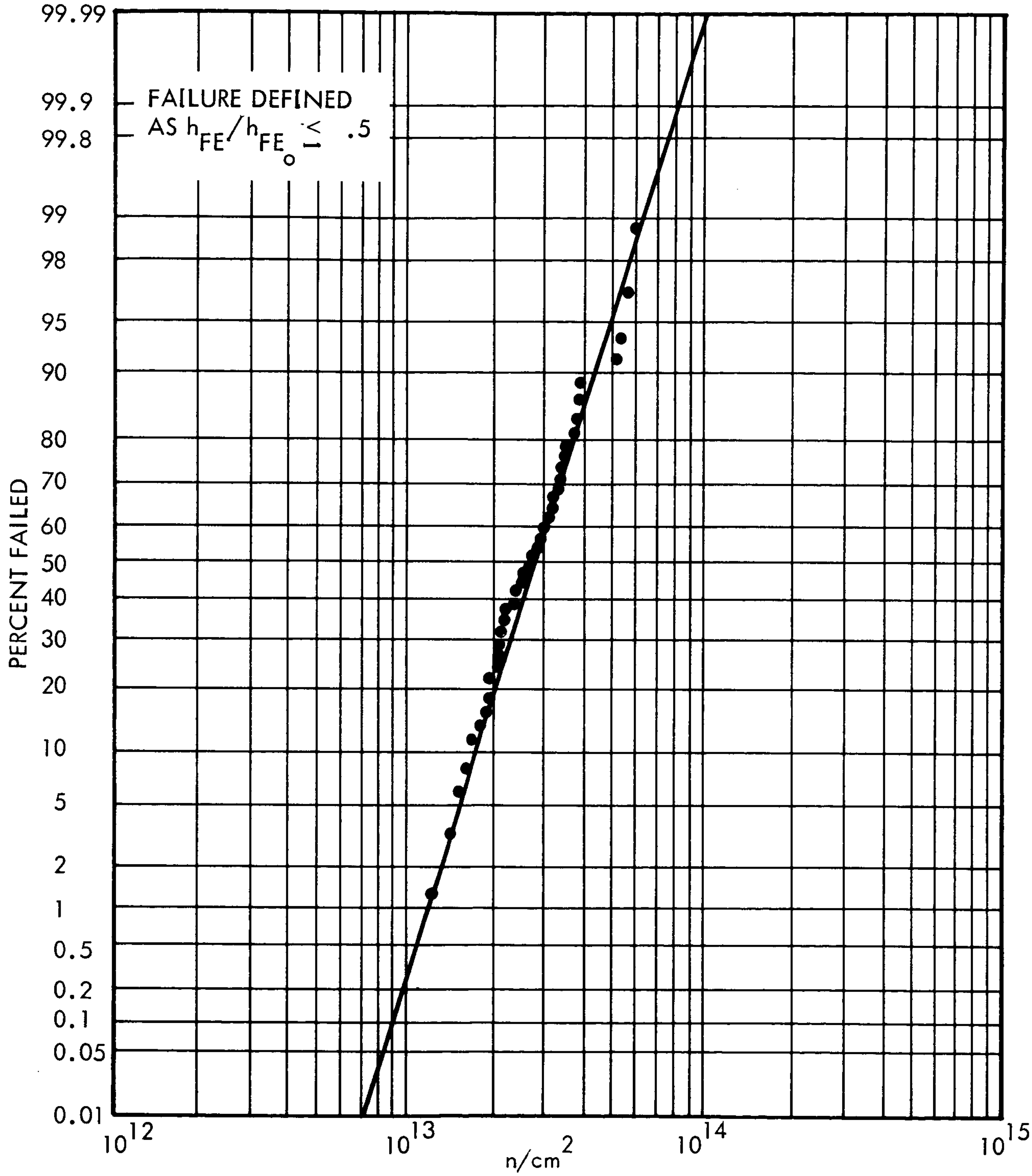

FIGURE 13 2N834, MOTOROLA, 45° C, PERCENT FAILED VERSUS INTEGRATED NEUTRON FLUX

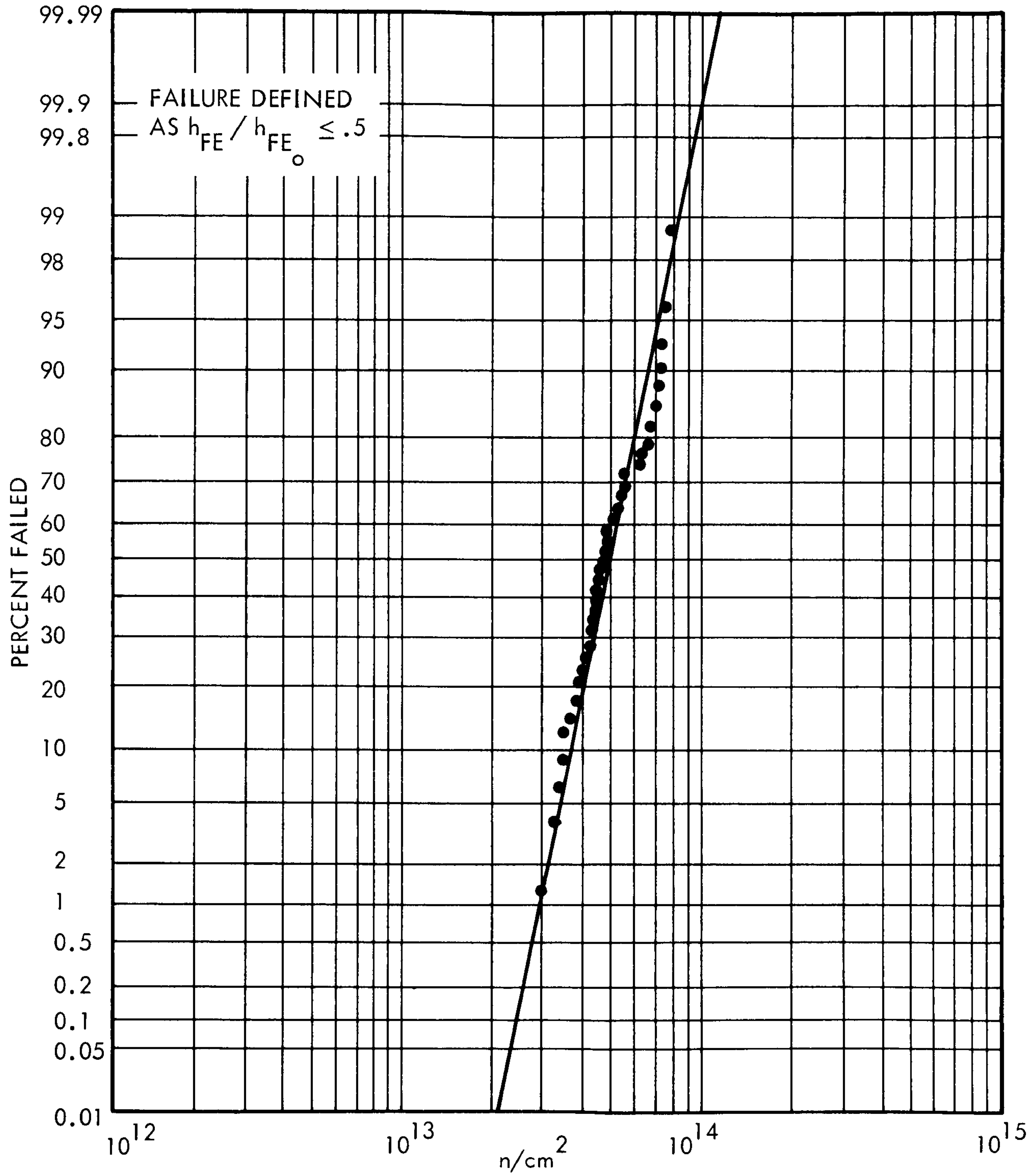

FIGURE 14 2N834, FAIRCHILD, 45° C, PERCENT FAILED VERSUS INTEGRATED NEUTRON FLUX

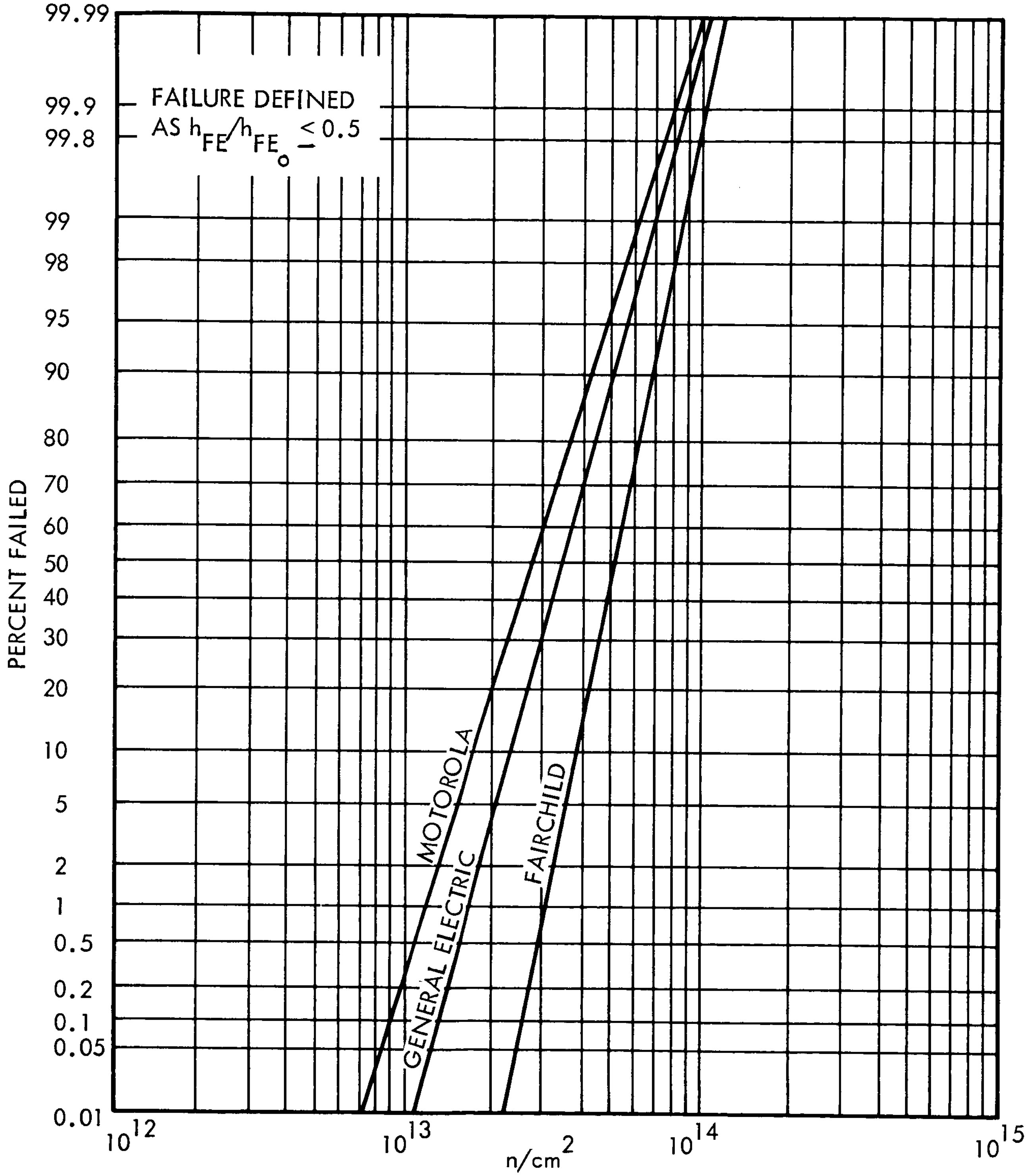

FIGURE 15 2N834, (GENERAL ELECTRIC, MOTOROLA AND FAIRCHILD), 45° C, PERCENT FAILED VERSUS INTEGRATED NEUTRON FLUX

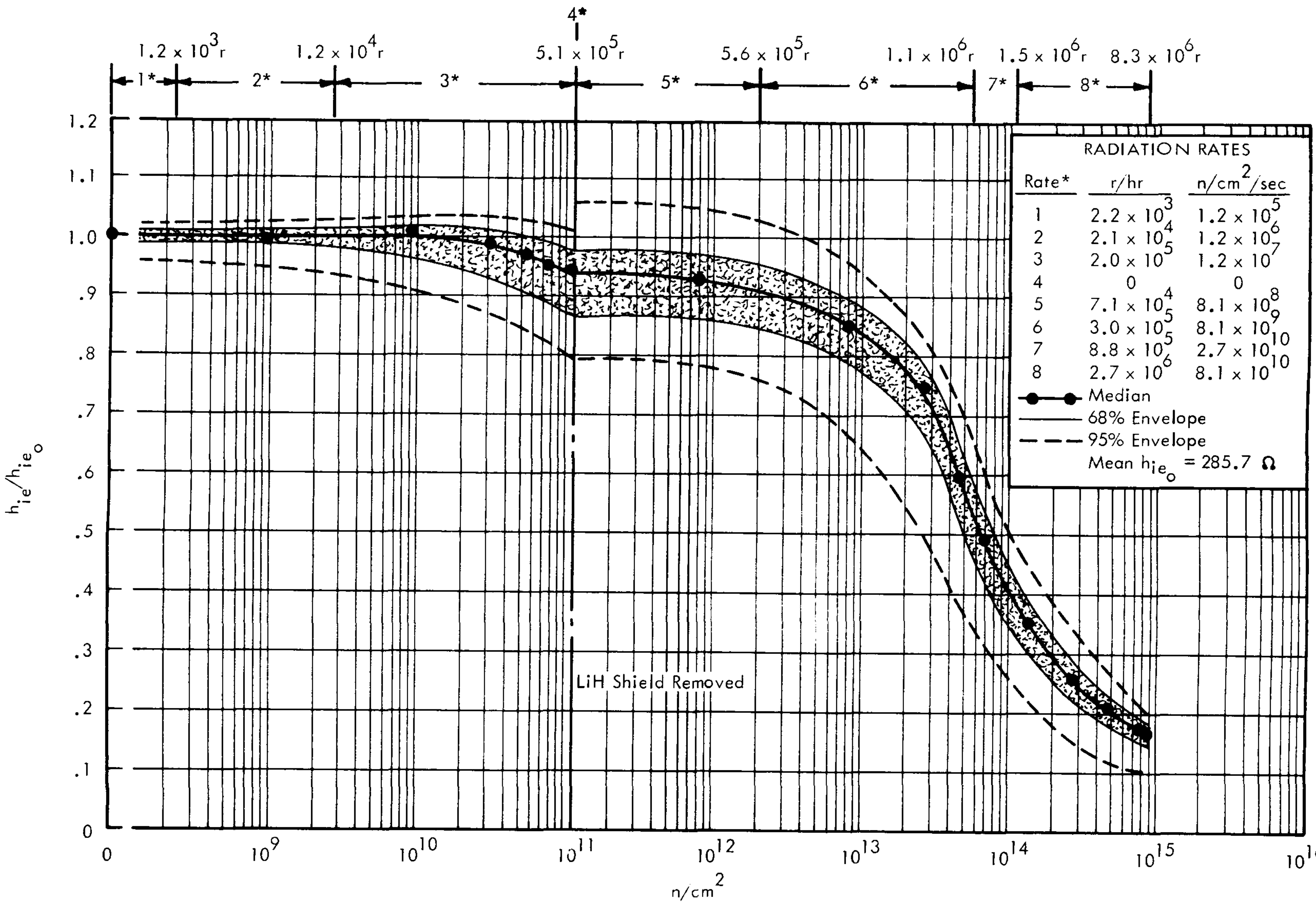

FIGURE 16 2N834, GENERAL ELECTRIC, 45° C, NORMALIZED h_{ie} VERSUS INTEGRATED NEUTRON FLUX

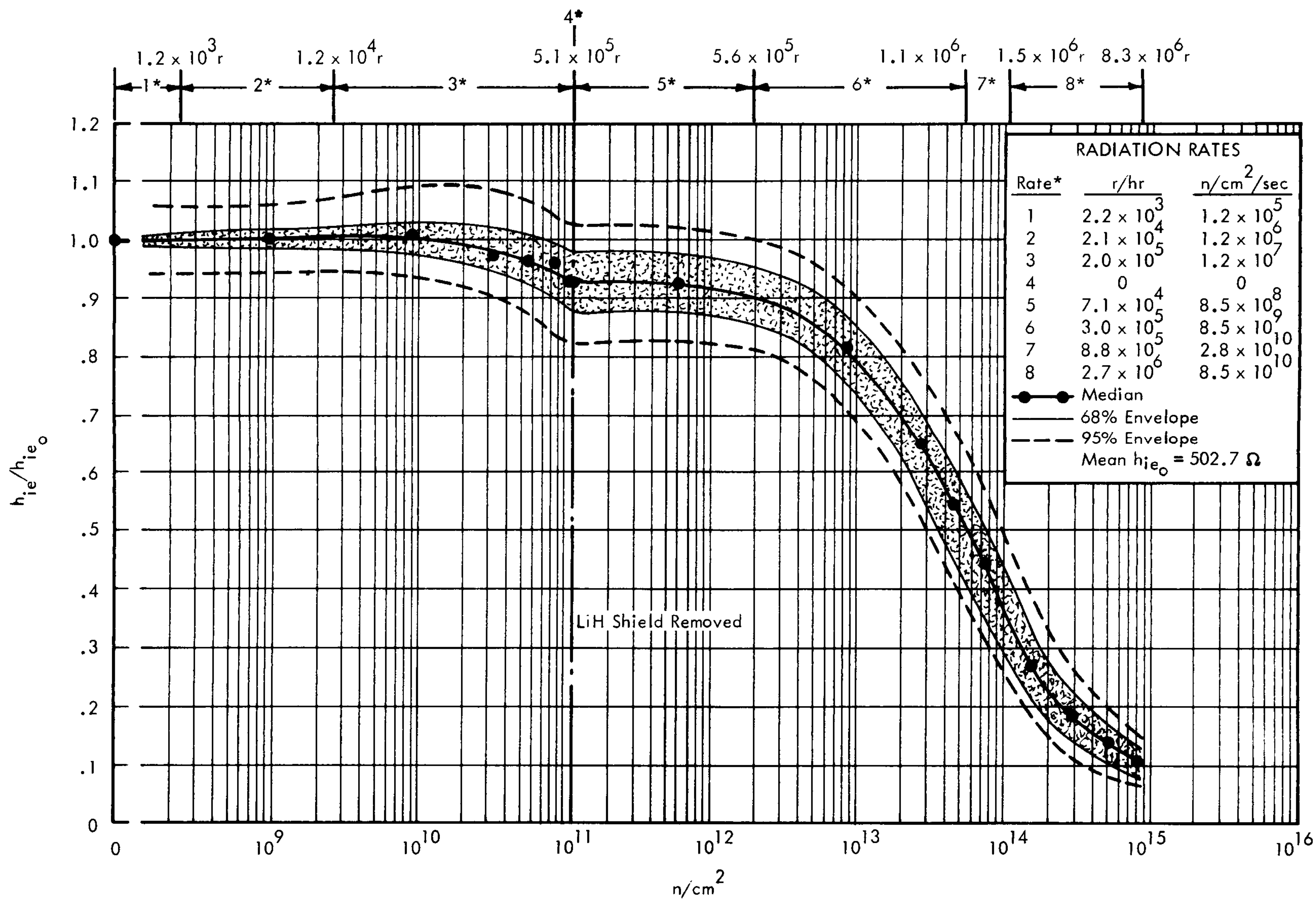

FIGURE 17 2N834, MOTOROLA, 45° C, NORMALIZED h_{ie} VERSUS INTEGRATED NEUTRON FLUX

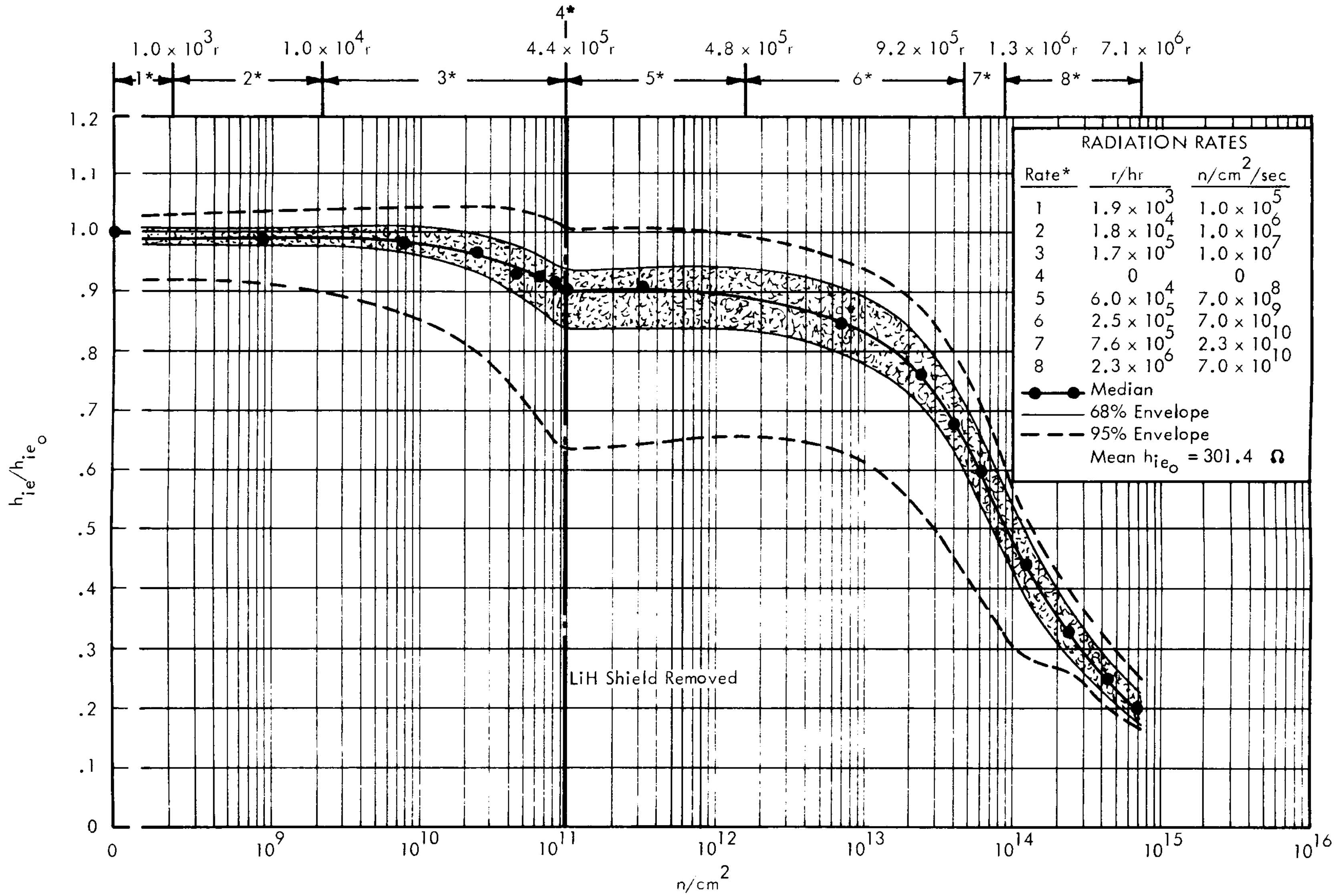

FIGURE 18 2N834, FAIRCHILD, 45° C, NORMALIZED h_{ie} VERSUS INTEGRATED NEUTRON FLUX

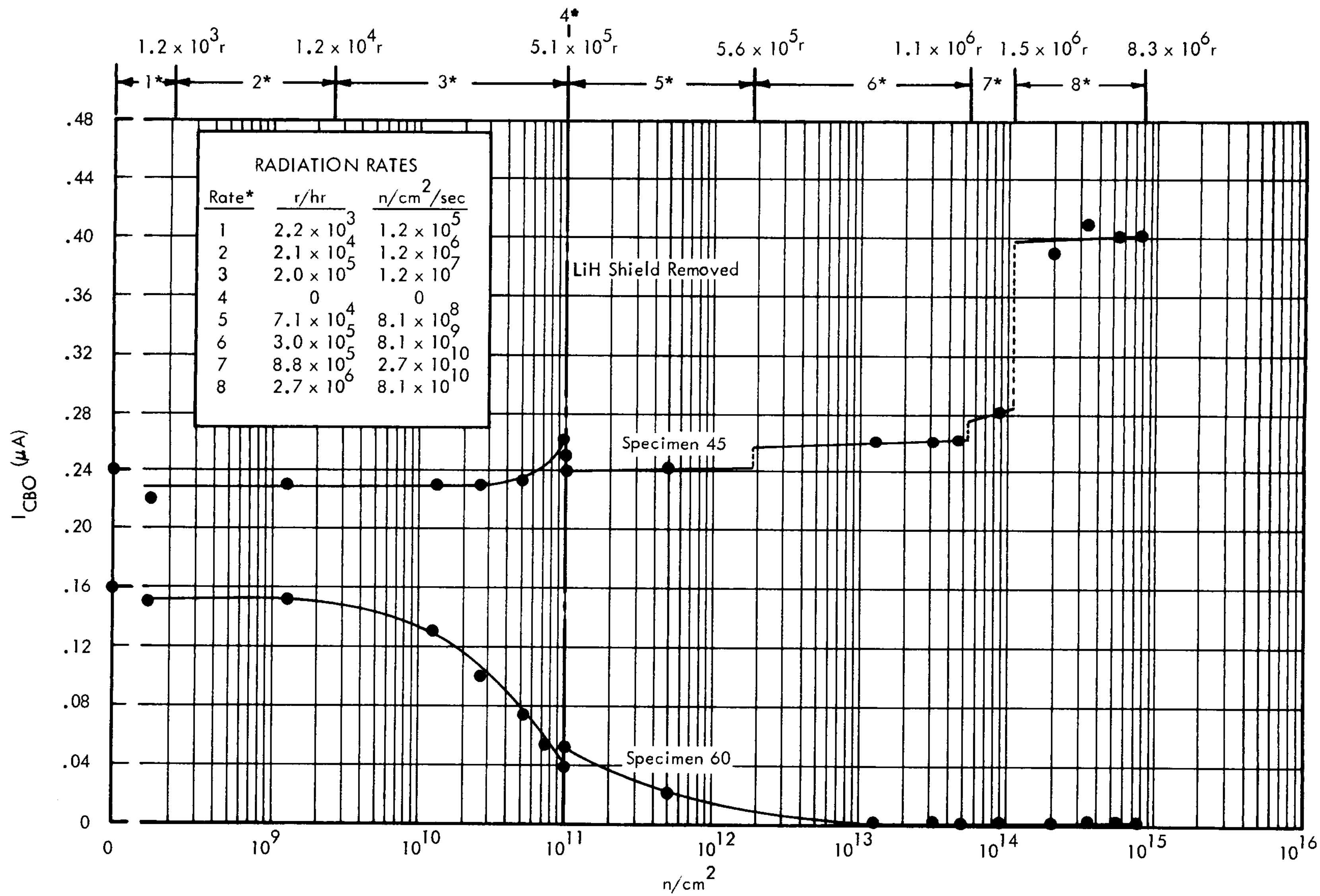

FIGURE 19 2N834, GENERAL ELECTRIC, (2 "UNUSUAL" SPECIMENS), 45° C, I_{CBO} VERSUS INTEGRATED NEUTRON FLUX

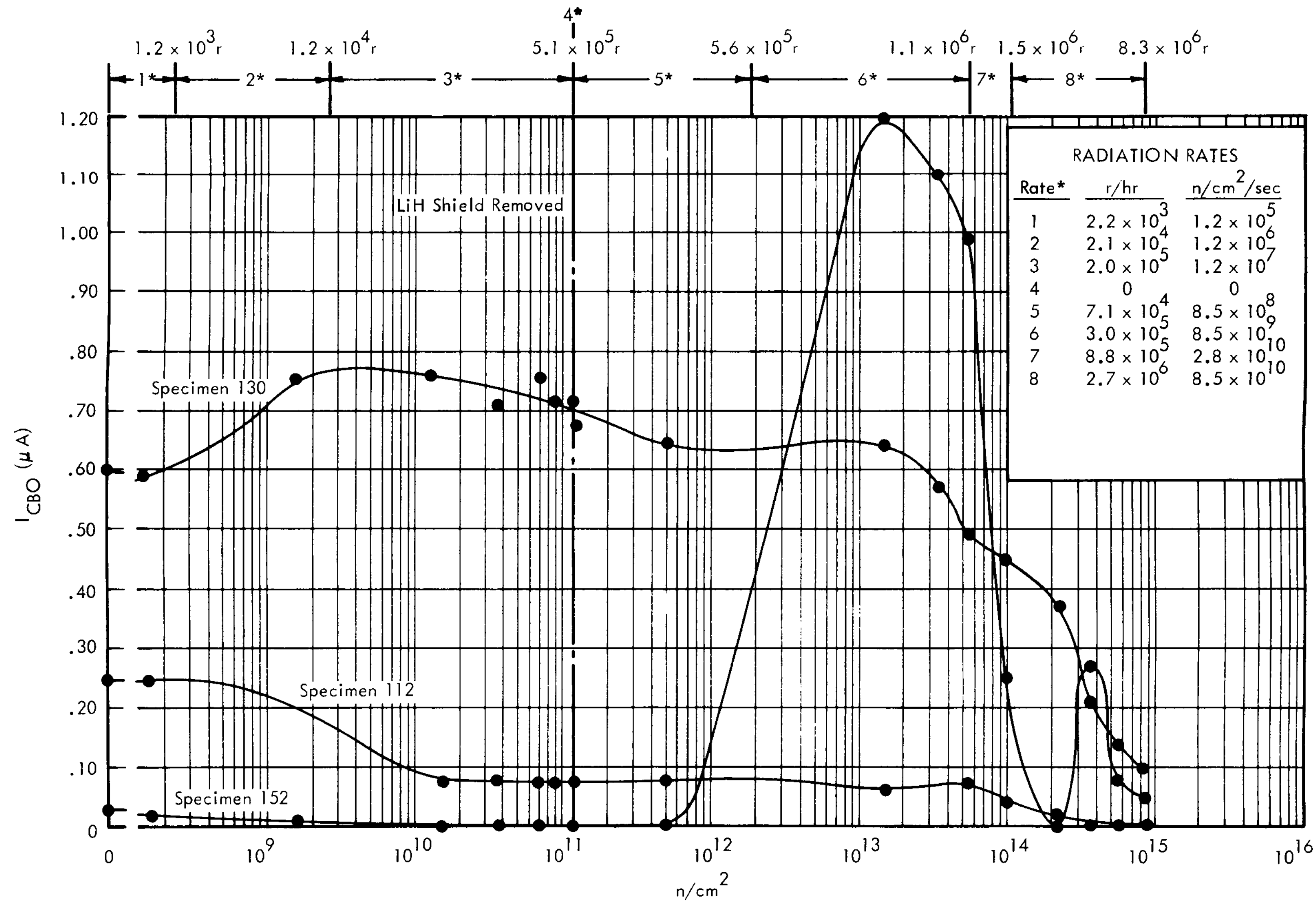

FIGURE 20 2N834, MOTOROLA, (3 "UNUSUAL" SPECIMENS), 45°C, I_{CBO} VERSUS INTEGRATED NEUTRON FLUX

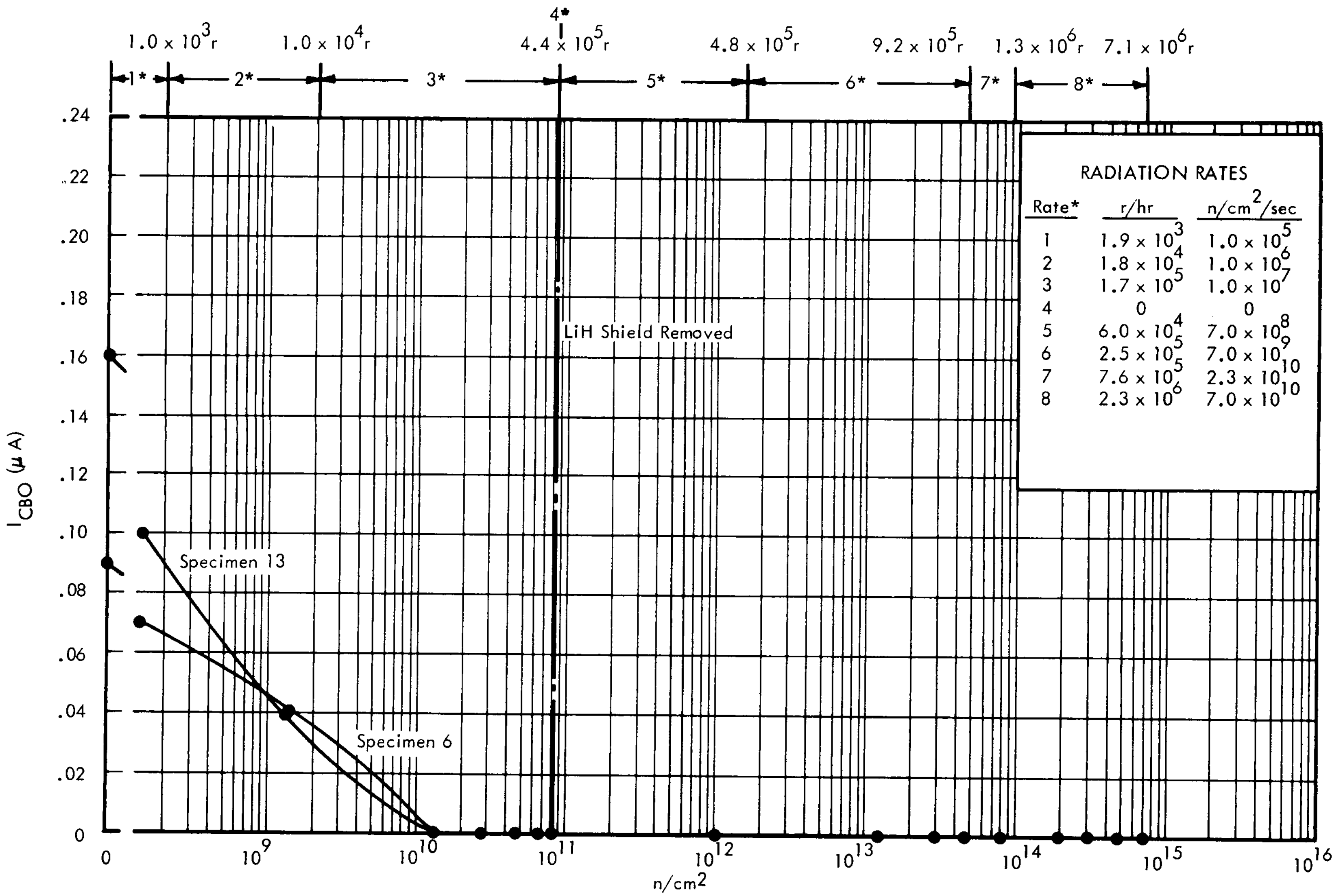

FIGURE 21 2N834, FAIRCHILD, (2 "UNUSUAL" SPECIMENS), 45° C, I_{CBO} VERSUS INTEGRATED NEUTRON FLUX

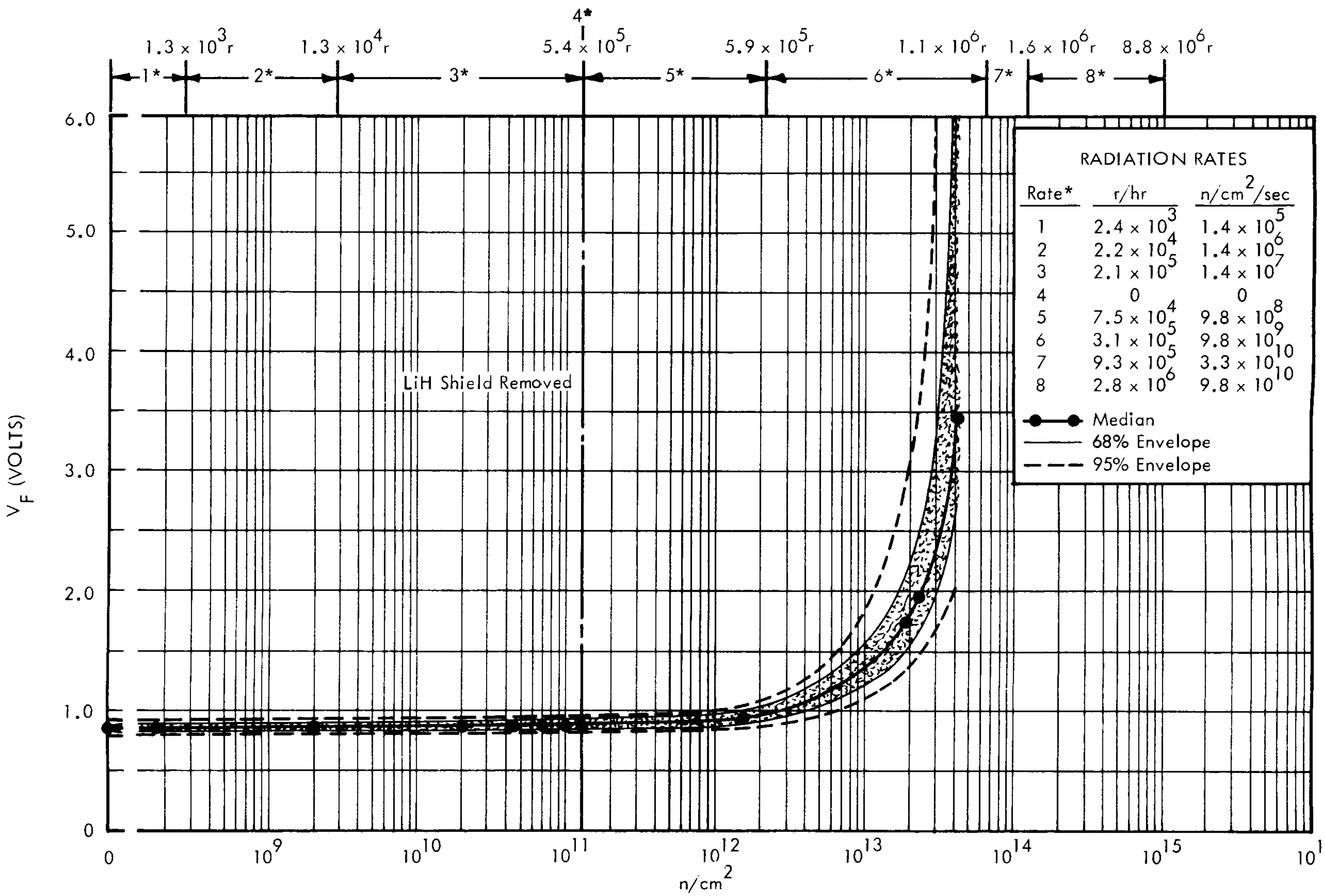

FIGURE 22 1N540, GENERAL ELECTRIC, 45° C, V_F (I_F = 250 mA) VERSUS INTEGRATED NEUTRON FLUX

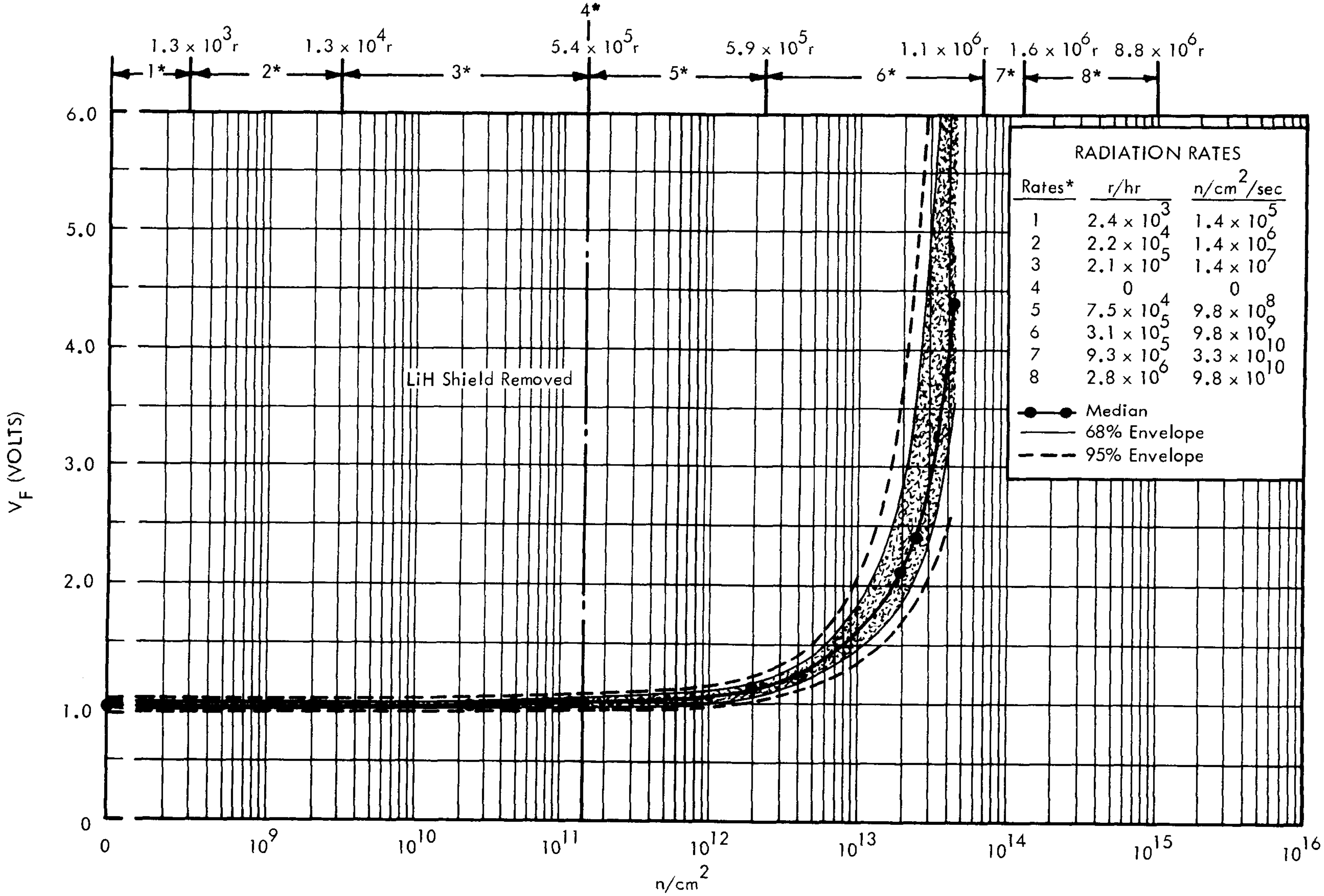

FIGURE 23 1N540, GENERAL ELECTRIC, 45° C, V_F (I_F = 500 mA) VERSUS INTEGRATED NEUTRON FLUX

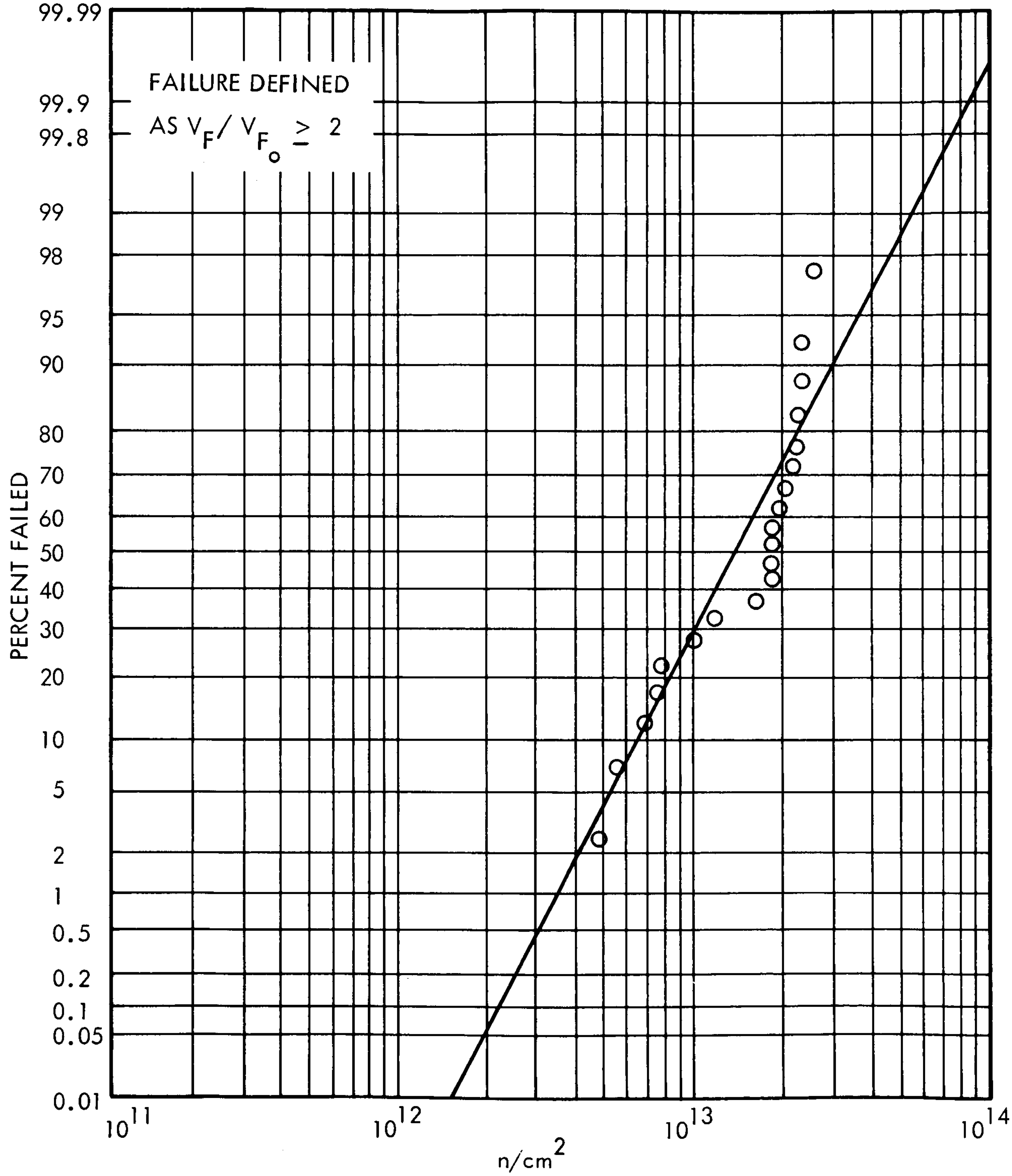

FIGURE 24 IN540, GENERAL ELECTRIC, I_F = 250 ma, 45° C, PERCENT FAILED VERSUS INTEGRATED NEUTRON FLUX

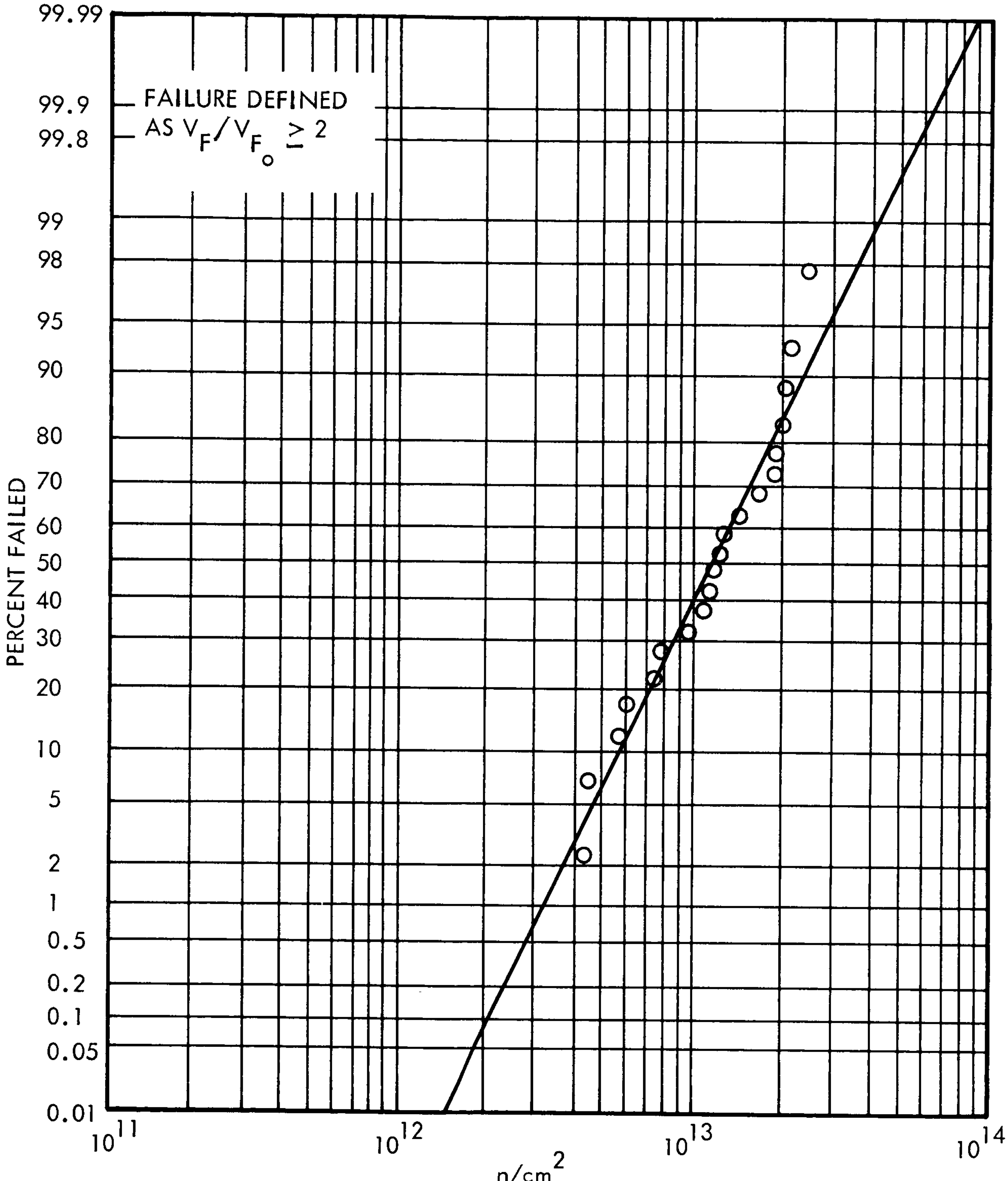

FIGURE 25 IN540, GENERAL ELECTRIC, I_F = 500 ma, 45° C, PERCENT FAILED VERSUS INTEGRATED NEUTRON FLUX

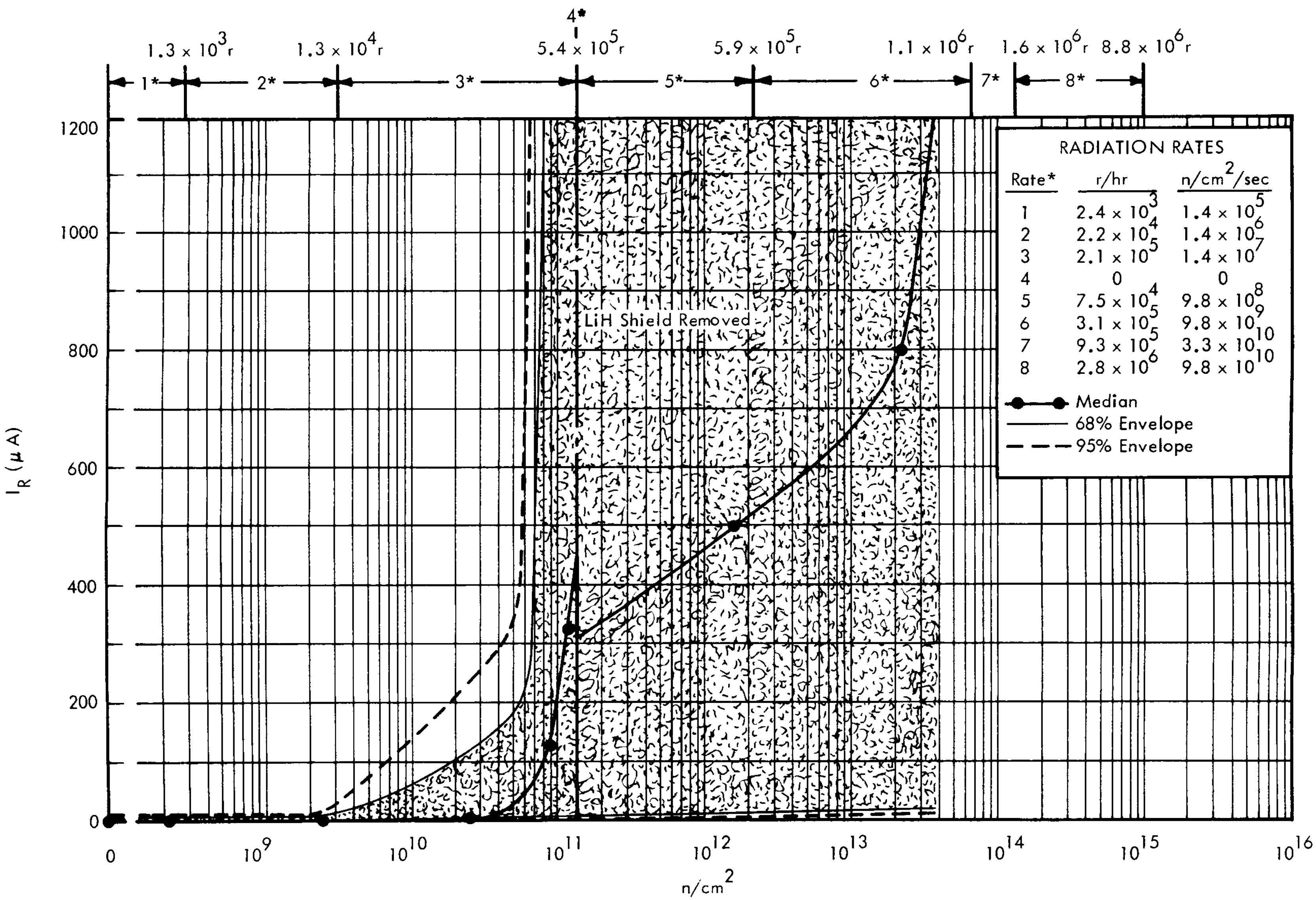

FIGURE 26 1N540, GENERAL ELECTRIC, 45° C, I_R (V_R = 400 VDC) VERSUS INTEGRATED NEUTRON FLUX

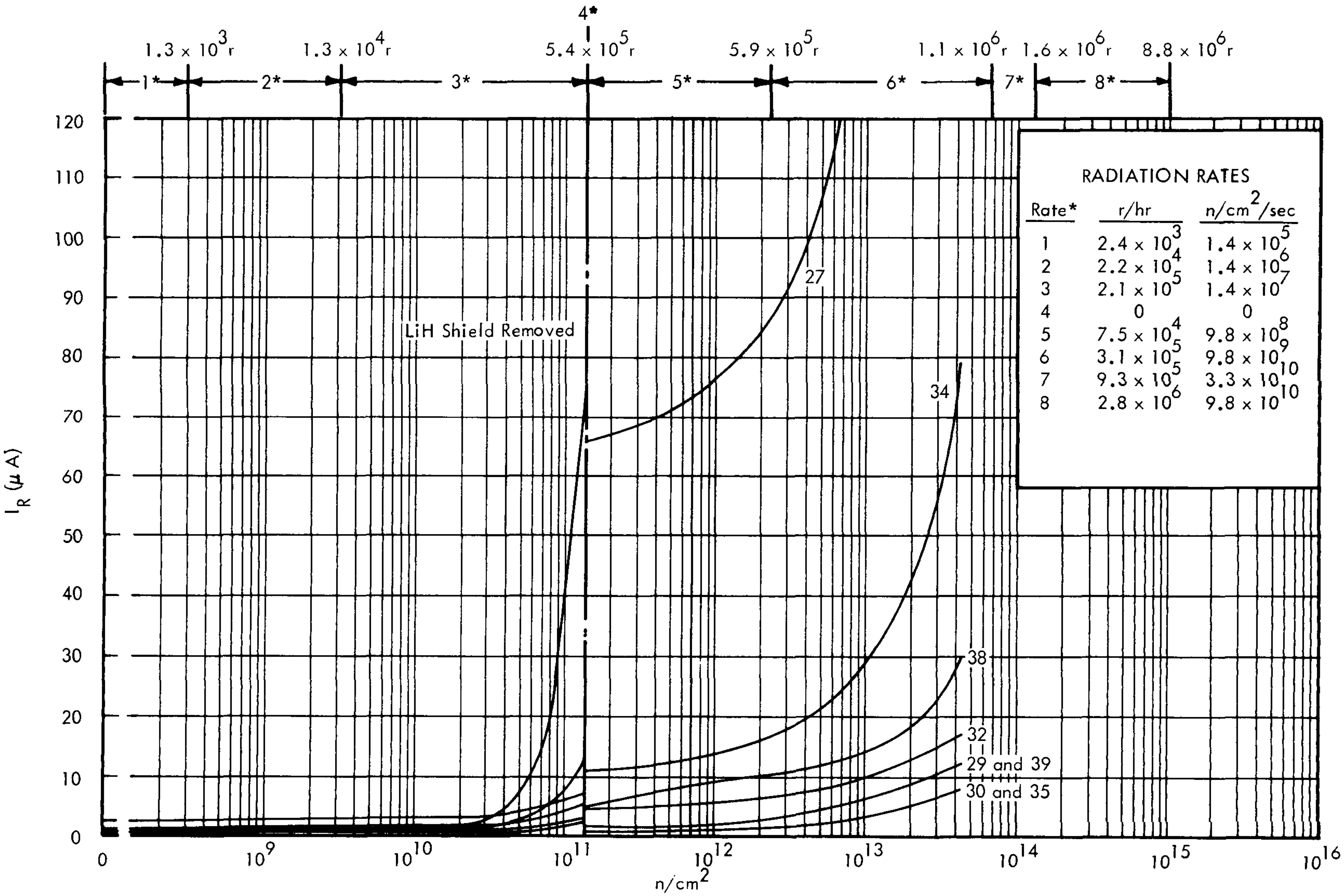

FIGURE 27 1N540, GENERAL ELECTRIC, (LOWER 8 SPECIMENS), 45° C, I_R (V_R = 400 VDC) VERSUS INTEGRATED NEUTRON FLUX

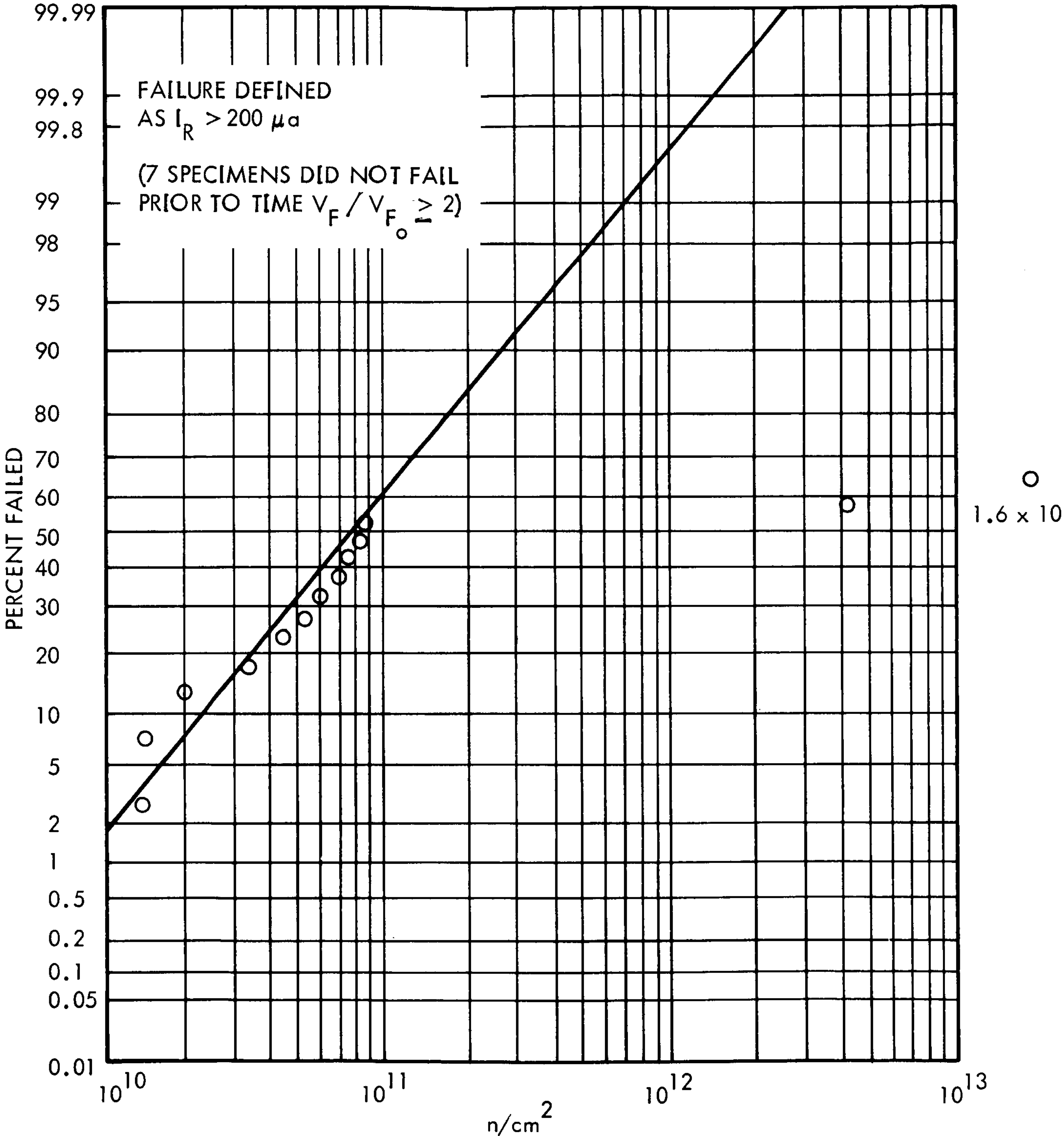

FIGURE 28 IN540, GENERAL ELECTRIC, 45° C, PERCENT FAILED VERSUS INTEGRATED NEUTRON FLUX

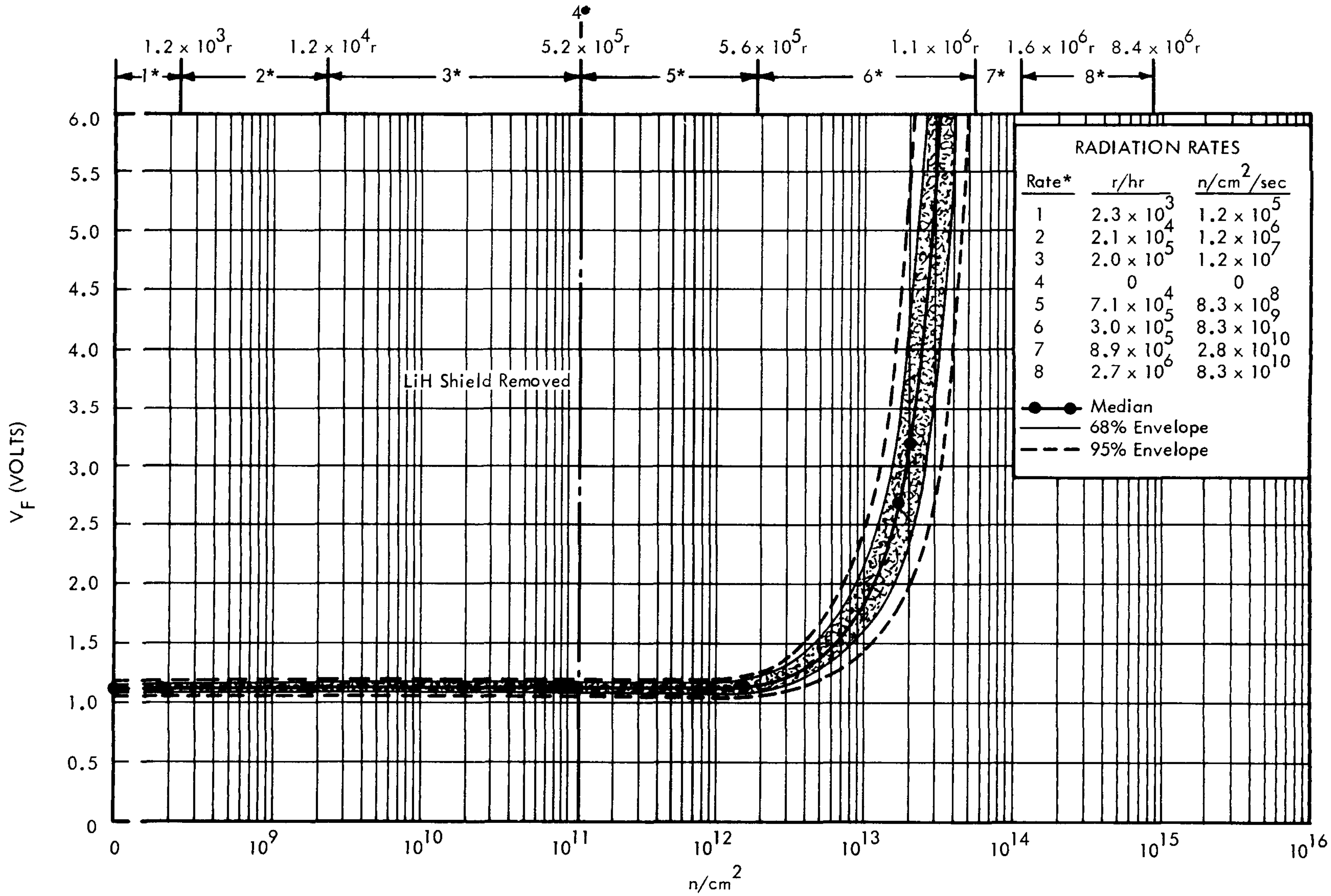

FIGURE 29 1N649, GENERAL ELECTRIC, 45° C, V_F (I_F = 200 mA) VERSUS INTEGRATED NEUTRON FLUX

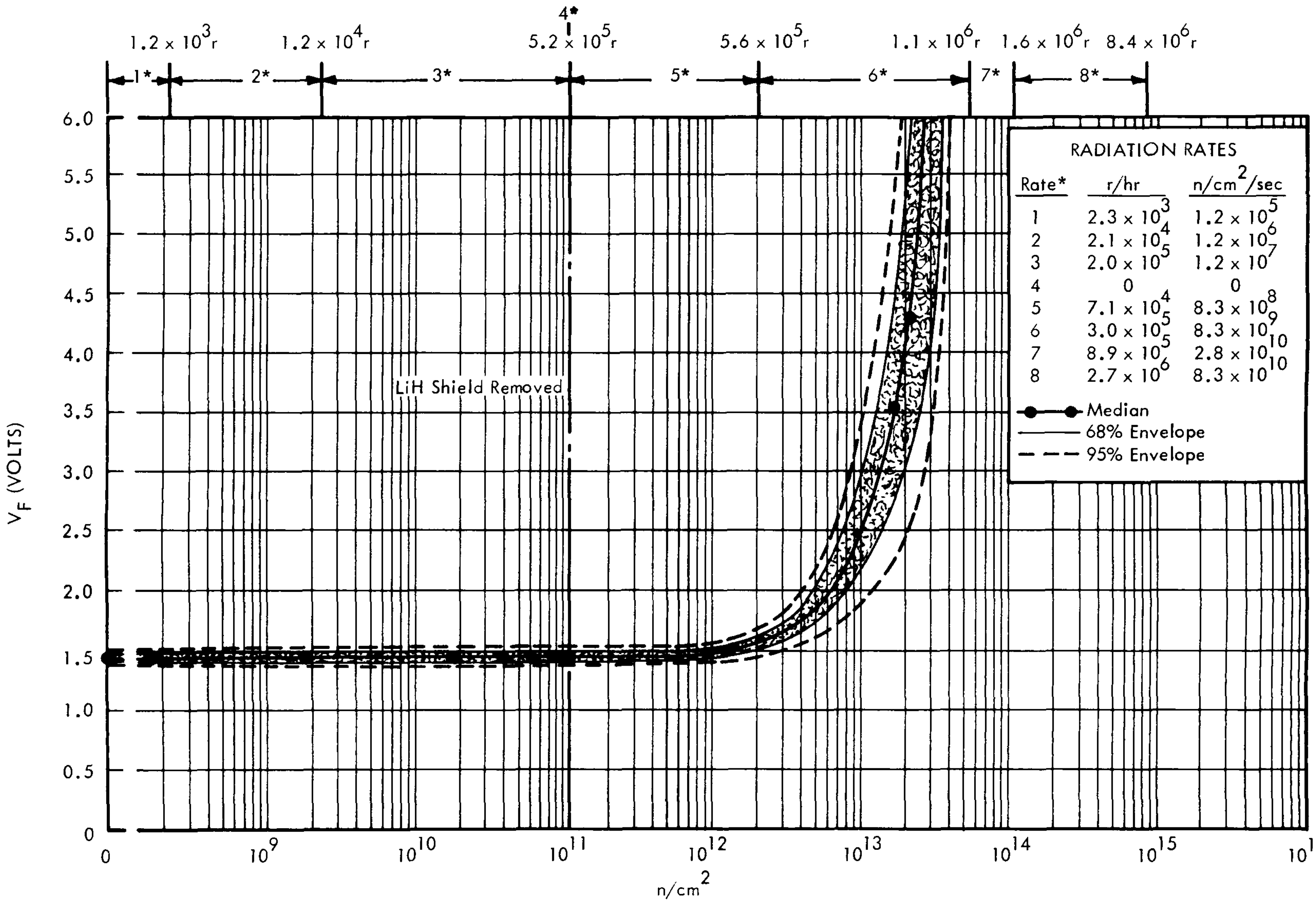

FIGURE 30 1N649, GENERAL ELECTRIC, 45° C, V_F (I_F = 400 mA) VERSUS INTEGRATED NEUTRON FLUX

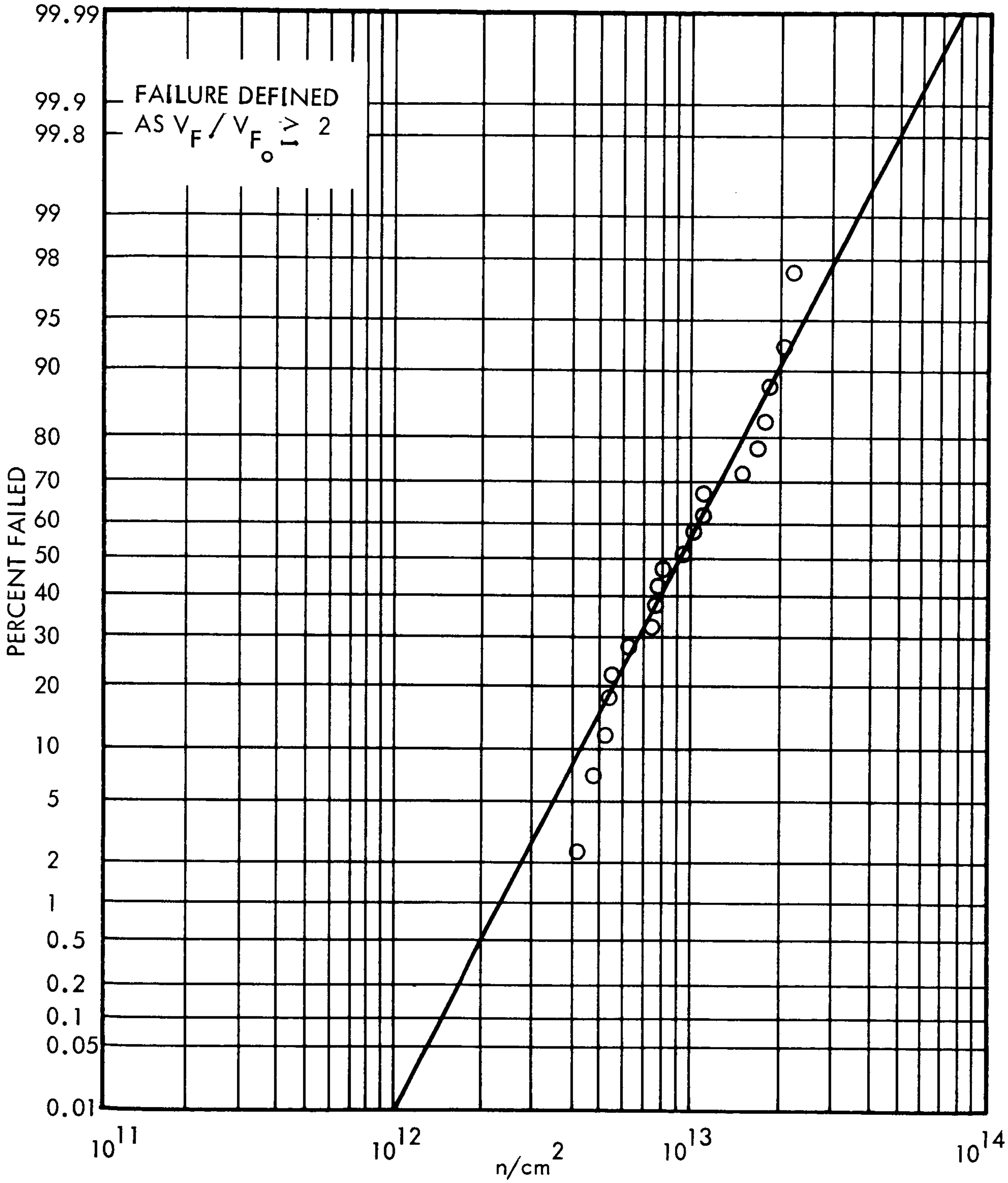

FIGURE 31 IN649, GENERAL ELECTRIC, I_F = 200 ma, 45° C, PERCENT FAILED VERSUS INTEGRATED NEUTRON FLUX

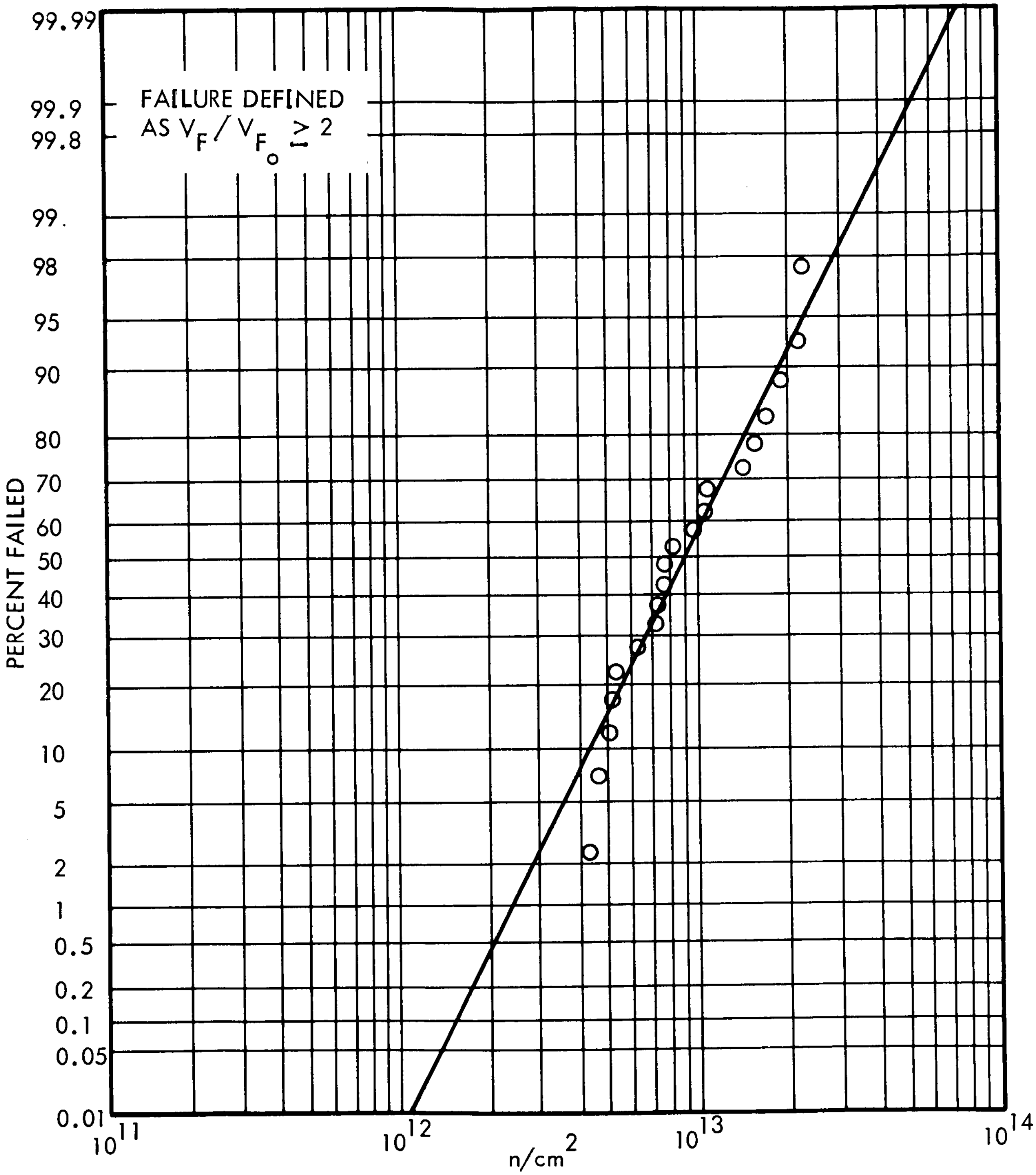

FIGURE 32 IN649, GENERAL ELECTRIC, I_F = 400 ma, 45° C, PERCENT FAILED VERSUS INTEGRATED NEUTRON FLUX

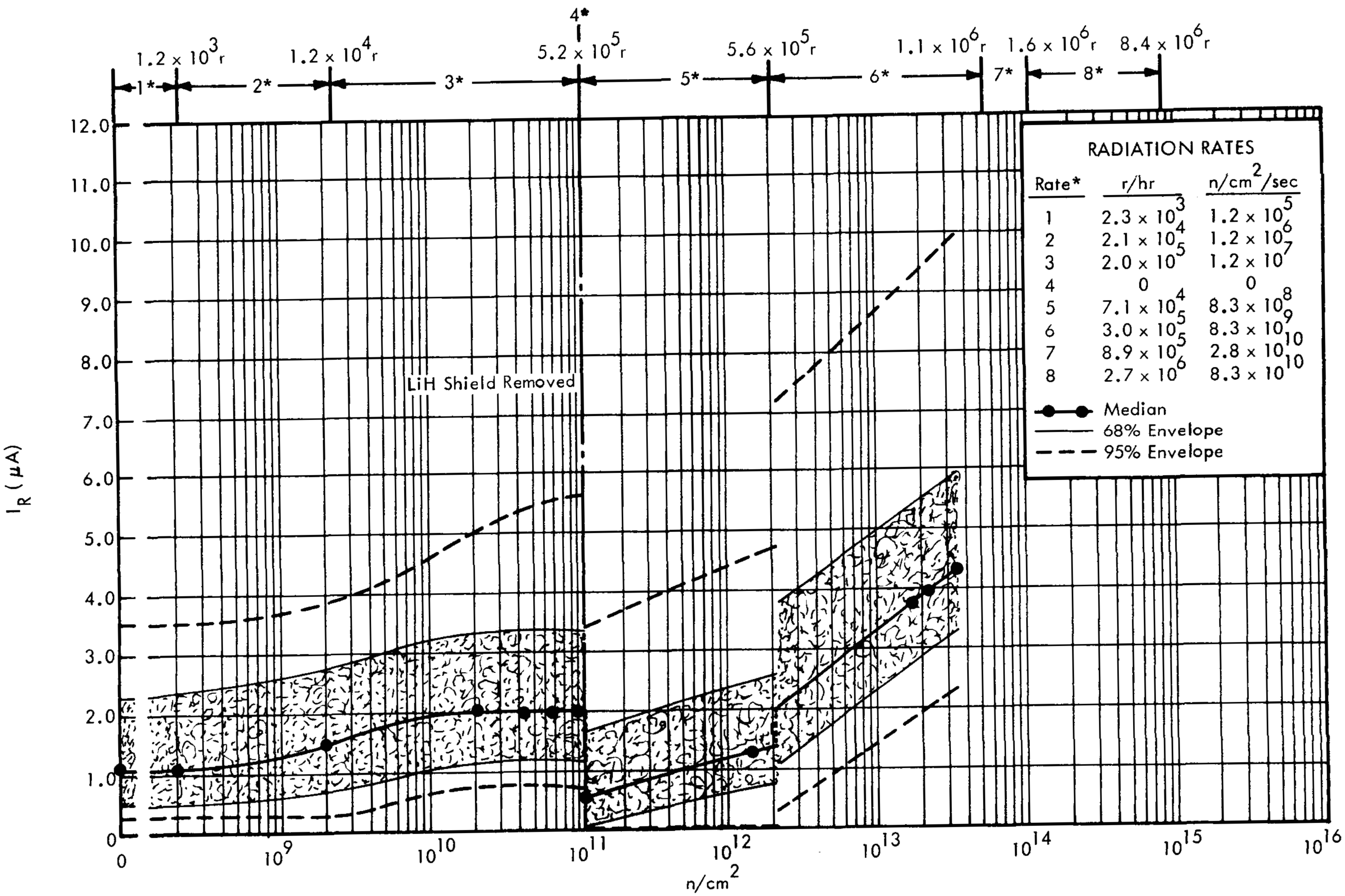

FIGURE 33 1N649, GENERAL ELECTRIC, 45° C, I_R (V_R = 400 VDC) VERSUS INTEGRATED NEUTRON FLUX

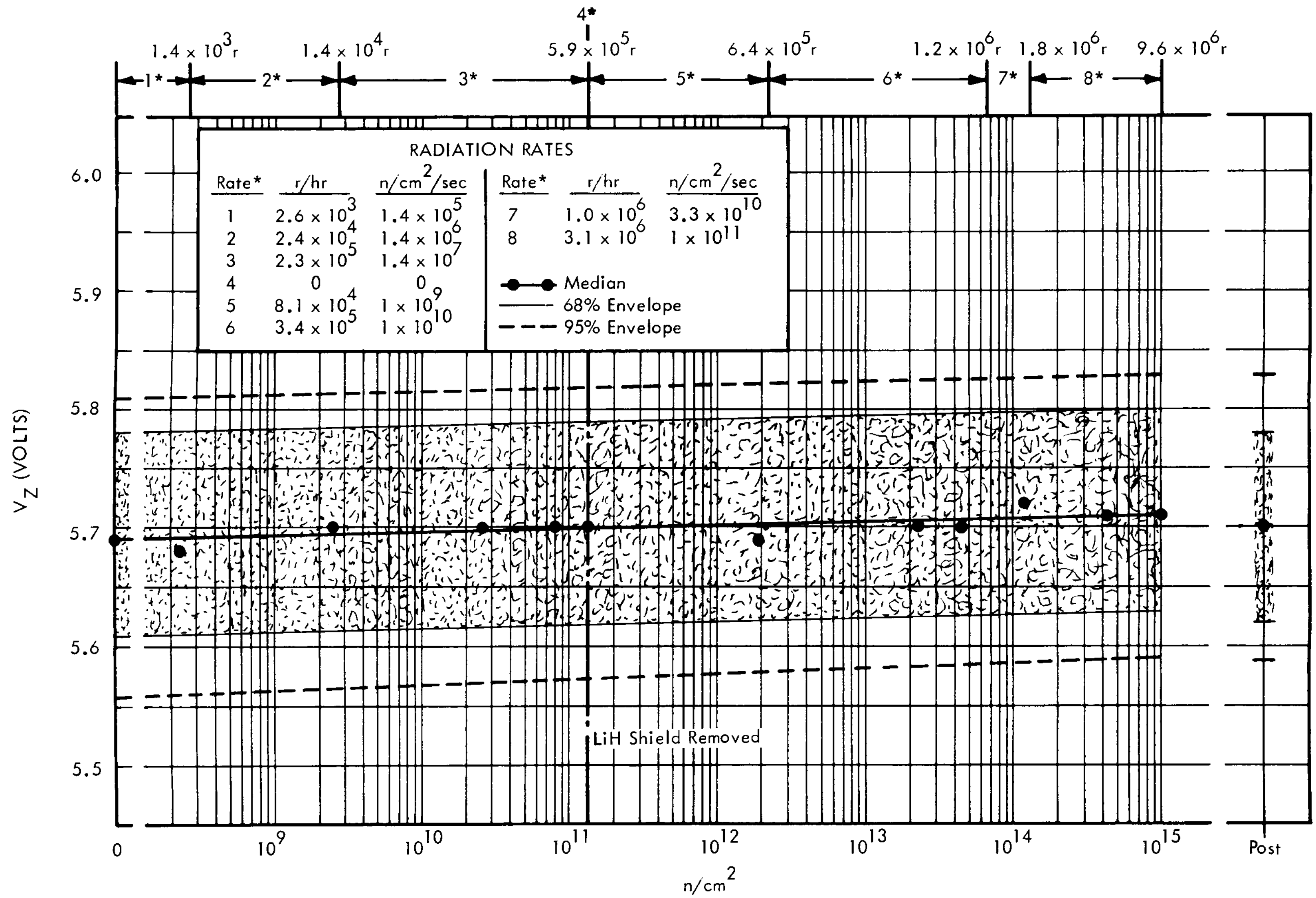

FIGURE 34 SIN752A, MOTOROLA, 45° C, V_Z VERSUS INTEGRATED NEUTRON FLUX